Tunnelling and Underground Space Technology 84 (2019) 413–431

Contents lists available at ScienceDirect

Tunnelling and Underground Space Technology

journal homepage: www.elsevier.com/locate/tust

A comprehensive solution for the calculation of ground reaction curve in the crown and sidewalls of circular tunnels in the elastic-plastic-EDZ rock mass considering strain softening

Ali Ghorbani*, Hadi Hasanzadehshooiili

Dept. of Civil Engineering, Faculty of Engineering, Univ. of Guilan, Rasht, Guilan, Iran

ARTICLE INFO

Keywords:
GRC
Elastic-plastic-EDZ
Unified criterion
Damaged zone

ABSTRACT

Although the determination of ground reaction curve (GRC) for tunnels has been extensively studied, formation of a damaged zone around the tunnel along with effects of some new features, including intermediate principle stress, exponential decaying dilation parameter, weight of the damaged rock and Young's modulus variation in the excavation damaged zone (EDZ) on the GRC development have not yet been considered. In this paper, considering all the affecting parameters including the previously studied ones and the new features, a comprehensive solution for the calculation of GRC of circular tunnels is presented. First, defining a more realistic medium for medium quality rock mass, behavior of tunnel's surrounding rock mass is categorized into elastic, plastic and excavation damaged zones, where materials in the plastic zone experience a strain softening. Also, rock mass through this strain softening, elastic-plastic-EDZ medium obeys Unified strength criterion (USC). Next, regarding the new defined medium, radial stress at the plastic-EDZ boundary is numerically calculated. Defining separate normalized radiuses for the plastic and damaged zones, thickness of annuluses, also, stress and strain increments are derived for different regions through finite difference solution of governing equilibrium and compatibility equations. The results of the proposed algorithm are verified using the field measurement data of Hanlingjie tunnel, China and its high accuracy is shown. Also, omitting the new features of the proposed algorithm, its comprehensiveness is discussed through comparison with some available solutions in the literature and a very good consistency is obtained. On the other hand, considering new features of the proposed algorithm, a considerable discrepancy is achieved indicating the importance of consideration of these features in the ground reaction curve development.

1. Introduction

Stresses and strains around tunnels have been extensively investigated as one of the major elements of tunnel design (Alejano et al., 2009, 2010; Alonso et al., 2003; Azadi and Hosseini, 2010; Brown et al., 1983; Carranza-Torres and Fairhurst, 1999; Carranza-Torres and Fairhurst, 2000; Ghorbani and Hasanzadehshooiili, 2017; González-Cao et al., 2013; Katzenbach et al., 2013). Also, Lee and Pietruszczak (2008), Park et al. (2008), Sharan (2008), Zareifard and Fahimifar (2016), Zhang et al. (2017) have studied such behaviors. These analyses are used to develop the ground reaction curve (GRC) of differently shaped tunnels constructed in rock masses of differing quality under different in-situ stress states. Due to the complexities of these problems, some of the complicated rock mass behaviors, in-situ stress states, and tunnel shapes cannot be analytically solved, and there is no straightforward, coupled, numerical-analytical solution to the problem. Indeed, different solution approaches (finite element, finite difference, discrete element, boundary element or combined methods, e.g., finite discrete element methods) to the rock mechanics and tunneling problems are available (Clausen, 2007; Ghorbani et al., 2013; Hamdi et al., 2014; Lee and Pietruszczak, 2008; Vrakas and Anagnostou, 2014) and these special types of problems can be solved using available commercial (FE, FD, BE, FDE, etc.) codes. Nevertheless, regarding the advantages of an independent analytical or coupled analytical-numerical solution method (e.g., the possibility of simply conducting parametric studies, validating constitutive models, validating numerical simulation stages using commercial codes, improving and applying developed codes for other scientific and research purposes, making modifications to source code to account for specific considerations, and benefitting from simplicity in modeling compared to the complicated design steps

* Corresponding author.
E-mail addresses: ghorbani@guilan.ac.ir (A. Ghorbani), h.hasanzadeh.shooiili@gmail.com, hasanzadeh@phd.guilan.ac.ir (H. Hasanzadehshooiili).

https://doi.org/10.1016/j.tust.2018.11.045
Received 17 June 2017; Received in revised form 26 August 2018; Accepted 25 November 2018
Available online 30 November 2018
0886-7798/

in commercial software packages), some simplifications are made to the original problem, and it has been further investigated analytically or coupled analytically-numerically (Alonso et al., 2003; Brown et al., 1983; Ghorbani and Hasanzadehshooiili, 2017; González-Cao et al., 2013; Zou et al., 2017; Lee and Pietruszczak, 2008; Park, 2014, 2015; Sharan, 2008; Vrakas and Anagnostou, 2014), also, (Wang et al., 2010; Zareifard and Fahimifar, 2014, 2016). Some of the related research is focused on the GRC of circular openings below groundwater level and investigation of the effects of seepage forces and pore water pressure on the response of the opening (Zareifard and Fahimifar, 2014), (Park, 2015) and (Vrakas and Anagnostou, 2014) studied the GRC for large strains in high squeezing rock masses using similarity solutions. But, the main focus of this paper is on circular openings in an isotropic rock mass under hydrostatic in-situ stress field that is experiencing infinitesimal strain increments and is constructed in a strain-softening, elastic-plastic-EDZ rock mass. To model the material's behavior, different strength criteria may be applied. Among the available solutions, some of them use the linear Mohr-Coulomb strength criterion (Alejano et al., 2009; Guan et al., 2007; Park, 2015; Zareifard and Fahimifar, 2014), and others implement the nonlinear Hoek-Brown strength criterion (Alejano et al., 2010; Carranza-Torres and Fairhurst, 1999, 2000; Zou et al., 2017; Mohammadi and Fahimifar, 2015; Park et al., 2008; Sharan, 2008). But, it is believed that nonlinear Unified criterion, considering the effect of intermediate principle stress, will better represent material's stress-strain behavior (Mohammadi et al., 2013; Xu and Yu, 2006; Yu et al., 2002; Zhang et al., 2010, 2012). Hence, Unified strength criterion is adopted to define the material's peak and residual stress-strain behaviors. Also, elastic-brittle-plastic, elastic-perfect plastic, and elastoplastic strain softening material behaviors are considered as the materials' constitutive laws in different analyses (Alonso et al., 2003; Brown et al., 1983; González-Cao et al., 2013; Lee and Pietruszczak, 2008; Park, 2014, 2015; Sharan, 2008; Wang et al., 2010; Zareifard and Fahimifar, 2014) Elastic-brittle-plastic behavior stands for hard rock masses with Geological Strength Index, *GSI*, values more than 75, while elastic-perfectly plastic behavior better represents the behavior of soft rock masses with *GSI* values lower than 25 (Alejano et al., 2009). Two first laws neglect the material softening, while the third model, accounting for the deterioration of material's strength parameters in the softening region, presents the behavior of a wider range of rock masses (medium rock mass with $25 < GSI < 75$), elastic-plastic behavior with strain softening. Moreover, to better interpret the post-peak behavior of rock masses and the relationship between radial and tangential plastic strain increments, more complicated dilatancy models should be applied (Alejano and Alonso, 2005; Alejano et al., 2009). Among the available solutions, (Alejano et al., 2009) and (Ketabian and Molladavoodi, 2015) considered such post-peak treatments, showing an exponential decay in the dilation parameter. However, as will be shown, these researchers do not consider the formation of an excavation damaged zone around the tunnel. Other available solutions assume a constant dilation parameter (Brown et al., 1983; Carranza-Torres and Fairhurst, 1999; Carranza-Torres and Fairhurst, 2000; Zou et al., 2017; Ghorbani and Hasanzadehshooiili, 2017; González-Cao et al., 2013; Mohammadi et al., 2013; Zareifard and Fahimifar, 2012, 2016) or provide a framework to supply dilation angle into the dilation parameter iteratively, and asses post-peak behavior with a linear decay in the dilation parameter (Lee and Pietruszczak, 2008; Mohammadi and Fahimifar, 2015; Park et al., 2008). In addition, as described, since tunneling is commonly conducted using one of the blasting or excavating methods, a damaged zone is formed around the blasted or excavated tunnel's section (González-Cao et al., 2013; Huang et al., 2016; Mohammadi et al., 2013; Zareifard and Fahimifar, 2016). The induced zone is generally described as the excavation damaged zone (EDZ), and the degree of induced damage as well as the radius of the damaged zone can be calculated using observation and classical methods (Anläggnings AMA 98, 1999) or quantified using the (García-Bastante et al., 2012) method based on Langefor's theory of blast calculation. Since the majority of rock masses surrounding the tunnels are medium rock masses, also, due to blasting operations, an excavation damaged zone is often formed around the tunnels, it is important to consider the elastoplastic stress-strain behavior and to consider the effects of variable post peak dilatancies and the material's softening in the plastic zone, as well as the effects of EDZ. Hence, this paper considers all of the important described elements. Regarding (Saiang, 2008a), the developed EDZ should consider the deterioration of the material's strength and stiffness parameters through EDZ (Saiang, 2008a). Also, taking the weight of crushed rock in EDZ into consideration will increase the accuracy of developed models. Among the developed solutions to the problem of ground reaction curve, only (González-Cao et al., 2013; Mohammadi et al., 2013; Zareifard and Fahimifar, 2016) considered the formation of EDZ around the tunnel in their models. Nevertheless, there remain some major shortcomings in the available solutions. In research conducted by Mohammadi et al. (2013), formation of the plastic zone is ignored, and an elastic-EDZ region is the domain of the problem. In González-Cao et al. (2013), although an efficient coupled self-similar-FE solution is applied to investigate the GRC of the circular tunnel in an elastic-plastic-EDZ rock mass, the deterioration of material stiffness and consideration of the weight of EDZ are not considered. Also not taken into account in their models are the effects of variable post peak dilatancies. Moreover, their proposed method uses the linear Mohr-Coulomb strength criterion, which is believed to have some shortcomings in the simulation of nonlinear stress-strain behaviors compared to the available nonlinear Hoek-Brown and unified strength criteria. Zareifard and Fahimifar (2016) suggested an elastic-plastic-EDZ rock mass behavior in their proposed closed-form solution, but their solution only covers elastic-brittle-plastic and elastic-perfectly-plastic material behaviors, and strain softening in the plastic zone was not considered. Moreover, as EDZ considerations, neither the weight of damaged rock nor the deterioration of the material's stiffness is considered. Table 1 presents a comprehensive literature survey on the problem of the ground reaction curve of circular tunnels in rock masses. In this table, the applied strength criteria and type of used flow rule, consideration of strain softening, and availability of an excavation damaged zone in all the studied cases are presented. Details of the considerations in EDZ also are presented.

Among the available solutions, some of the presented studies propose a closed-form solution to the problem thanks to simplifications made to the original problem (Sharan, 2008; Zareifard and Fahimifar, 2016). Others apply numerical or semi-analytical methods. These studies generally use two different solution approaches: some of them apply a self-similar solution to obtain the values of tunnel convergence against different internal support pressures (Alejano et al., 2009, 2010; Alonso et al., 2003; González-Cao et al., 2013; Park, 2014, 2015). The second group follows a sequential and iterative solution scheme for the solution of their problem (Brown et al., 1983; Zou et al., 2017; Ketabian and Molladavoodi, 2015; Lee and Pietruszczak, 2008; Mohammadi and Fahimifar, 2015; Park et al., 2008; Wang et al., 2010; Zareifard and Fahimifar, 2012). In this group, Zou et al. (2017) uses a different treatment with the normalized radius to update stresses and correspondingly calculate strains. In addition, some intelligent methods have also been applied to obtain ground reaction curve. (Ghorbani and Hasanzadehshooiili, 2017) (2017) used the evolutionary polynomial regression and neural network methods to develop some new relationships for both the Mohr-Coulomb and Hoek-Brown strain softening material models based on available solutions (Ghorbani and Hasanzadehshooiili, 2017; Ghorbani et al., 2018).

Because there have not been many studies on the ground reaction curve of tunnels in elastic-plastic-EDZ rock masses, this paper presents a comprehensive study in which many parameters of concern are considered. In order to comprehensively investigate the ground reaction curve of a circular tunnel, an iterative finite difference procedure similar to the method applied in Lee and Pietruszczak (2008) is used and

Table 1
A literature survey on the ground reaction curve problem of circular tunnels.

Research	Concerning parameters						
	Failure criterion	Flow rule	Exponential decaying dilation	Strain softening	EDZ considerations		
					Weakened strength parameters	Weight of EDZ	Varying Young's modulus
Brown et al. (1983)	H-B	assoc.	×	√	×	×	×
Carranza-Torres and Fairhurst (1999)	H-B	non-assoc.	×	×	×	×	×
Carranza-Torres and Fairhurst (2000)	H-B	non-assoc.	×	×	×	×	×
Alonso et al. (2003)	M-C & H-B	non-assoc.	×	√	×	×	×
Mitaim and Detournay (2005)	Duncan-Chang	non-plastic	×	×	×	×	×
Xu and Yu (2006)	Unified	non-assoc.	×	×	×	×	×
Guan et al. (2007)	M-C	assoc.	×	√	×	×	×
Sharan (2008)	H-B	assoc.	×	×	×	×	×
Park et al. (2008)	H-B	non-assoc.	×	√	×	×	×
Lee and Pietruszczak (2008)	M-C & H-B	non-assoc.	×	√	×	×	×
Alejano et al. (2009)	M-C	non-assoc.	√	√	×	×	×
Wang et al. (2010)	M-C & H-B	non-assoc.	×	√	×	×	×
Zhang et al. (2010)	Unified	non-assoc.	×	×	×	×	×
Alejano et al. (2010)	H-B	non-assoc.	×	√	×	×	×
Serrano et al. (2011)	M-C & H-B	non-assoc.	×	×	×	×	×
Wang and Yin (2011)	M-C & H-B	non-assoc.	×	×	×	×	×
Zareifard and Fahimifar (2012)	H-B	non-assoc.	×	√	×	×	×
Zhang et al. (2012)	Unified	non-assoc.	×	×	×	×	×
Mohammadi et al. (2013)	Unified	non-assoc.	×	×	√	×	×
González-Cao et al. (2013)	M-C	non-assoc.	×	√	√	×	×
Vrakas and Anagnostou (2014)	M-C	non-assoc.	×	×	×	×	×
Zareifard and Fahimifar (2014)	M-C	non-assoc.	×	×	×	×	×
Park (2014)	M-C & H-B	non-assoc.	×	√	×	×	×
Park (2015)	M-C	non-assoc.	×	×	×	×	×
Mohammadi and Fahimifar (2015)	H-B	non-assoc.	×	√	×	×	×
Ketabian and Molladavoodi (2015)	M-C & H-B	non-assoc.	√	√	×	×	×
Zareifard and Fahimifar (2016)	M-C & H-B	non-assoc.	×	×	√	×	×
Ghorbani and Hasanzadehshooiili (2017)	M-C & H-B	non-assoc.	×	√	×	×	×
Zou et al. (2017)	M-C & H-B	non-assoc.	×	√	×	×	×
Present study	Unified	non-assoc.	√	√	√	√	√

Note: M-C = Mohr-Coulomb strength criterion; H-B = Hoek-Brown strength criterion; Unified = Unified Strength Criterion; assoc. = associative flow rule; non-assoc. = non-associative flow rule; √ = considered; × = not considered.

is extended to the EDZ using some newly derived relationships. The nonlinear Unified Strength Criterion (USC) is adopted, and the effect of strain softening in the plastic zone is considered. This strength criterion considers the effects of intermediate principle stress, which are not addressed in the original Mohr-Coulomb or Hoek-Brown criteria. In fact, the Hoek-Brown failure criterion can be considered as a special case for Unified criterion in which the effect of intermediate principle stress is not considered. As shown in Table 1, the new proposed method models the elastic-plastic-EDZ behavior of the surrounding rock mass in the which material's strength parameters and stiffness deterioration, and the weight of the damaged zone in EDZ are considered. Post-peak variable dilatancy models presented by Alejano and Alonso (2005) and Alejano et al. (2009) are also considered to cover a wide range of the material's behavior. Unlike previous available solutions, the new solution makes it possible to comprehensively consider all the parameters that affect GRC when required data is available for modeling purposes.

2. Problem definition and methodology

A circular tunnel in a continuous isotropic elastic-plastic-EDZ rock mass, which is under far field hydrostatic stress, σ_0, is depicted in Fig. 1, where an internal support pressure of is exerted on the tunnel boundary. In Fig. 1, b_i is the tunnel radius, and R_{EDZ} and R_P, respectively, present the radius of the excavation damaged zone and the

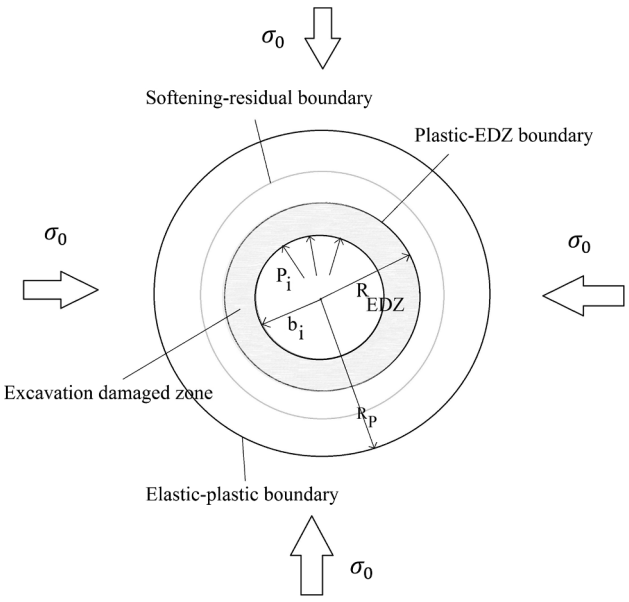

Fig. 1. Definition of different regions formed around a circular tunnel.

plastic zone. In such cases, with decreasing internal support pressure, the formation of radial displacements initiates in the tunnel boundary. It continues to elastically deform until the support pressure reaches a critical value called critical support pressure, P_{ic} (Lee and Pietruszczak, 2008; Park et al., 2008); this value has a closed form solution for linear Mohr-Coulomb strength criterion (Brown et al., 1983) and is found numerically by using the Newton-Raphson algorithm for Hoek-Brown criterion (Lee and Pietruszczak, 2008; Park et al., 2008; Zareifard and Fahimifar, 2012). In this paper, like the Hoek-Brown case, the Newton-Raphson method is applied to obtain the critical support pressure for the case of Unified strength criterion. For internal support pressures less than critical support pressure and progressing toward the tunnel's face, the plastic stresses and strains occur. Stresses and strains in the plastic zone first follow a strain softening behavior and continue to progress in a residual way. The transition between softening and residual behaviors is controlled using a critical deviatoric plastic strain parameter, γ^{p*} (Abbasi et al., 2014; Alejano et al., 2010; Alonso et al., 2003; Ghorbani and Hasanzadehshooiili, 2017; Zou et al., 2017; Lee and Pietruszczak, 2008; Park et al., 2008). Progressing toward the tunnel face, an excavation damaged zone is formed. Radial stress in the plastic-EDZ boundary is found numerically using a proper Runge-Kutta-Fehlberg method (Mathews and Fink, 2004) and controls the stage of the solution. For radial stress larger than the plastic-EDZ boundary's radial stress, σ_r^{P-E}, the problem remains in the plastic region, follows a solution like the Lee and Pietruszczak (2008), and continues to reach the boundary value. For radial stress lower than σ_r^{P-E} , the problem uses outputs of the last stage in the plastic zone as the initial conditions, and proposes a new solution for the excavation damaged zone. Basics and main governing elements of the problem are presented in the following sections.

2.1. Unified yield criterion

Among developed rock strength criteria, those that track the principle stress-strain incremental paths in a non-linear way are largely applied and believed to more efficiently predict the behavior of materials (Alejano et al., 2010; Alonso et al., 2003; Carranza-Torres and Fairhurst, 1999, 2000; Hasanzadehshooiili et al., 2012; Hoek and Brown, 1997; Lee and Pietruszczak, 2008; Park et al., 2008; Sharan, 2008; Mohammadi and Fahimifar, 2015), also, (Veiskarami et al., 2012; Zareifard and Fahimifar, 2012). Regarding (Xu and Yu, 2006; Yu et al., 2002; Zhang et al., 2012), intermediate principle stress plays an important part in the radius of the excavation damaged zone. Hence, adopting a failure criterion, which accounts for the effect of intermediate principle stress, will result in better predictions of material behavior. Yu et al. (2002), based on true triaxial compression tests and the generalized form of the Hoek-Brown failure criterion, and considering intermediate principle stress, presented the Unified Strength Criterion (USC). Eqs. (1)–(3) show the generalized form of USC in a polar coordinate system (Yu et al., 2002; Zhang et al., 2010).

$$\sigma_\theta = \sigma_r + Y\left(m_b\frac{\sigma_r}{\sigma_c} + s\right)^a \tag{1}$$

$$Y = \frac{2(b+1)}{(2+b)}\sigma_c \tag{2}$$

$$b = \frac{(\sigma_c+\sigma_t)\tau_0 - \sigma_t\sigma_c}{(\sigma_t-\tau_0)\sigma_c} 0 \le b \le 1 \tag{3}$$

where σ_θ is the maximum principle stress (tangential stress) and σ_r is the minimum principle stress (radial stress). m_b, s, and a represent Hoek-Brown strength parameters for rock mass. And, b is a material parameter, which reflects the effect of intermediate principle stress and is calculated experimentally using true triaxial tests. It varies from 0 (the criterion will be changed into generalized form of Hoek-Brown criterion) to 1 (generalized Twin shear stress criterion is formed). In addition, σ_c, σ_t, and τ_0, respectively, show the uniaxial compressive strength, uniaxial tensile strength, and shear strength of rock material, and Y is an intermediate parameter used to define the effect of b parameter (Yu et al., 2002; Zhang et al., 2010).

To apply plasticity rules, the Unified strength criterion is assumed as the yield function. In addition to principle maximum and minimum stresses, materials' yielding is a function of the deviatoric plastic strain parameter, γ^p, which controls materials' strength parameters. This parameter is also called strain softening parameter (Lee and Pietruszczak, 2008; Park et al., 2008). Hence, the general form of the yield function is as following:

$$F(\sigma_\theta, \sigma_r, \gamma^p) = \sigma_\theta - \sigma_r - H(\sigma_r, \gamma^p) \tag{4}$$

$$H(\sigma_r, \gamma^p) = \frac{2(b(\gamma^p)+1)}{(2+b(\gamma^p))}\sigma_c(\gamma^p)\left(m_b(\gamma^p)\frac{\sigma_r}{\sigma_c(\gamma^p)} + s(\gamma^p)\right)^{a(\gamma^p)} \tag{5}$$

where Eq. (5) is calculated combining Eqs. (1)–(3) and (4). The strain softening parameter, γ^p, controls the transition of strength parameters in the plastic zone. It is not generally believed that there is a unique approach for defining this parameter (Alejano et al., 2009, 2010; Alonso et al., 2003; Brown et al., 1983; Ghorbani and Hasanzadehshooiili, 2017; Lee and Pietruszczak, 2008; Mohammadi and Fahimifar, 2015; Park et al., 2008; Sharan, 2008; Wang et al., 2010), and, (Zareifard and Fahimifar, 2012). Nevertheless, it is commonly defined as Eq. (6) (Lee and Pietruszczak, 2008; Park et al., 2008). This paper also uses Eq. (6) to define the softening behavior of rock mass and the transition of strength parameters in the plastic region.

$$\gamma^p = \varepsilon_\theta^p - \varepsilon_r^p \tag{6}$$

where ε_θ^p is the tangential plastic strain and ε_r^p declares the radial plastic strain.

2.2. Plastic potential function

Definition of a proper plastic potential function is one of the important factors affecting the progress of plastic strains. Indeed, since the relationship between radial and tangential plastic strain increments is defined by the flow rule, considering an associated or non-associated flow rule significantly affects the material's plastic behavior in the plastic zone. In this paper, the non-associated flow rule is used to model the relationship between radial and tangential plastic strain increments. Plastic potential function can be defined in different ways. The Mohr-Coulomb and Hoek-Brown similar forms of plastic potential are generally applied and implemented in computational geo-mechanics (Clausen, 2007).

2.2.1. Mohr-Coulomb similar type of plastic potential function

One of the most demanding forms of plastic potential function commonly used by rock mechanics engineers is the function presented in Eq. (7), which is generally similar in form to the Mohr-Coulomb strength criterion (Alejano et al., 2009).

$$G(\sigma_\theta, \sigma_r, \gamma^p) = \sigma_\theta - k(\gamma^p)\sigma_r \tag{7}$$

The peak value of k in Eq. (7) is computed using Eq. (8) (Alejano et al., 2009).

$$k_p = \frac{1+sin(\Psi_p)}{1-\sin(\Psi_p)} \tag{8}$$

where Ψ_p represents peak dilation angle observed in the elastic-plastic boundary and is calculated using the following equation (Alejano et al., 2010):

$$\Psi_p = \frac{5GSI_{peak} - 125}{1000}\varphi_p \tag{9}$$

The value of φ_p in Eq. (9), peak friction angle in the elastic-plastic boundary, is computed using Eq. (10), originally proposed by Hoek et al. (2002)

$$\varphi_p = \arcsin\left(\frac{6a_p m_p (s_p + m_p \sigma_r^{'})^{a_p-1}}{2(1+a_p)(2+a_p) + 6a_p m_p (s_p + m_p \sigma_r^{'})^{a_p-1}}\right) \tag{10}$$

$$\sigma_r^{'} = \frac{\sigma_R}{\sigma_c} \tag{11}$$

2.2.2. Hoek-Brown similar type of plastic potential function

As other authenticated plastic potential function, the general form presented in Eq. (12) is applied as the plastic potential function similar to the Hoek-Brown strength criterion (Clausen, 2007).

$$G(\sigma_\theta, \sigma_r, \gamma^p) = \sigma_\theta - \sigma_r - \sigma_c(\gamma^p)\left(m_g(\gamma^p)\frac{\sigma_r}{\sigma_c(\gamma^p)} + s_g(\gamma^p)\right)^{a_g(\gamma^p)}. \tag{12}$$

where m_g, s_g, and a_g are material parameters associated with the plastic potential function.

2.2.3. Definition of relationship between radial and tangential plastic strain increments

The general form of the relationship between radial and tangential plastic strain increments is presented below (Ghorbani and Hasanzadehshooiili, 2017; Ketabian and Molladavoodi, 2015; Lee and Pietruszczak, 2008; Park et al., 2008; Zareifard and Fahimifar, 2012):

$$d\varepsilon_r^p = -k(\gamma^p) d\varepsilon_\theta^p \tag{13}$$

where the relationship for $k(\gamma^p)$ is different for M-C and H-B similar forms of the plastic potential function. Eqs. (14), and (15), respectively, present the variable $k(\gamma^p)$ parameter for M-C (Alejano and Alonso, 2005) and H-B (Clausen, 2007) types of the plastic potential function.

$$k(\gamma^p) = 1 + (k_p - 1)e^{-\frac{\gamma^p}{\gamma^{p*}}} \tag{14}$$

$$k(\gamma^p) = 1 + a_g(\gamma^p) m_g(\gamma^p)\left(m_g(\gamma^p)\frac{\sigma_r}{\sigma_c(\gamma^p)} + s_g(\gamma^p)\right)^{a_g(\gamma^p)-1} \tag{15}$$

These two formulas present variable post-peak dilatancy behaviors: decaying form of dilation parameter presented in Eq. (14) for M-C type and variable plastic potential parameters for H-B type of plastic potential. But, in the case of constant dilation rate, the curvature parameter in Eq. (15), $a_g(\gamma^p)$, must be equal to 1. Hence, $k(\gamma^p)$ equation will be simplified into Eq. (16) (Clausen, 2007).

$$k(\gamma^p) = 1 + m_g(\gamma^p) \tag{16}$$

The corresponding case for M-C type of plastic potential function (constant dilation rate) will be $k(\gamma^p) = k_p$.

In this paper, regarding the availability of the required data for comparison purposes, Mohr-Coulomb similar type of plastic potential function is used for further studies. Next, using this function, some investigations are conducted on different dilation (no dilation, constant dilation, linear and exponential decaying dilations) and softening behaviors, also, softening initiation (different critical softening parameters).

2.3. Strength parameters in different zones

As illustrated earlier, materials' strength parameters are different in various zones. In the elastic zone, peak strength parameters for an intact rock mass are used to evaluate the stress-strain behavior of materials surrounding the tunnel. All the strength parameters in the plastic zone, which are functions of deviatoric plastic strain parameter, γ^p, are calculated using Eq. (17) (Alejano et al., 2009, 2010; Alonso et al., 2003; Ghorbani and Hasanzadehshooiili, 2017; González-Cao et al., 2013; Lee and Pietruszczak, 2008; Mohammadi and Fahimifar, 2015; Park et al., 2008; Zareifard and Fahimifar, 2012).

$$\omega(\gamma^p) = \begin{cases} \omega_p - (\omega_p - \omega_r)\frac{\gamma^p}{\gamma^{p*}} & 0 < \gamma^p < \gamma^{p*} \\ \omega_r & \gamma^p \geq \gamma^{p*} \end{cases} \tag{17}$$

where ω is a representative for each of the σ_c, σ_t, τ_0, m, s, a, m_g, s_g, a_g, and Ψ parameters. In addition, p and r subscripts respectively declare peak and residual values of studied parameters.

Also, the value of γ^{p*} for each of the parameters and every level of confinement stress is obtained experimentally using the method proposed by Alejano et al. (2010) as below:

$$\gamma^{p*} = \left(1 - \frac{1}{2}k_p\right)[\sigma_\theta^{peak}(\sigma_{r_{mean}}) - \sigma_\theta^{res}(\sigma_{r_{mean}})]\left[\frac{1}{E} + \frac{1}{M}\right] \tag{18}$$

$$\sigma_{r_{mean}} = \frac{P_{icr} + \sigma_r^{P-E}}{2} \tag{19}$$

$$\begin{cases} M = E\,[0.0046e^{0.0768GSI_p}]\left(\frac{\sigma_{r_{mean}}}{\sqrt{s_p}\sigma_c}\right)^{-1} & for \ \ \frac{\sigma_{r_{mean}}}{\sqrt{s_p}\sigma_c} > 0.1 \\ M = E\,[0.0046e^{0.0768GSI_p}]\left(\frac{\sigma_{r_{mean}}}{2\sqrt{s_p}\sigma_c} + 0.05\right)^{-1} & for \ \ \frac{\sigma_{r_{mean}}}{\sqrt{s_p}\sigma_c} \leq 0.1 \end{cases} \tag{20}$$

where M is the drop modulus used to characterize stress-strain behavior in Alejano et al. (2010). Also, $\sigma_\theta^{peak}(\sigma_{r_{mean}})$ and $\sigma_\theta^{res}(\sigma_{r_{mean}})$ are respectively calculated using Eq. (1) for peak and residual strength parameters. E is the material's Young's modulus. Regarding Eq. (17), material's behavior in plastic zone follows the first line of Eq. (17) for a strain softening parameter less than γ^{p*}. Also, the residual parameters are used when $\gamma^p \geq \gamma^{p*}$. Material's residual strength parameters are calculated using replacing the values for GSI_p with GSI_r and following the same procedure available for calculation of peak strength parameters. GSI_r can be calculated using Eq. (21) (Alejano et al., 2012).

$$GSI_r = 17.25e^{0.0107GSI_p} \tag{21}$$

Saiang (2008a) characterized the excavation damaged zone and the parameters induced by excavation or blasting. This research proposed a monotonic reduction in Young's modulus of material in EDZ. And as a simple quantifying method, Hoek et al. (2002) proposed a disturbance factor, D, to account for the effect of damaged zone on the strength parameters of the material. Also, the method presented by Anläggnings AMA 98 (1999) is an approximate method to calculate the material's parameters and the radius of the excavation damaged zone in EDZ. Moreover, the method of García-Bastante et al. (2012) developed based on Langefor's theory of blast calculation can also be used in this regard. Hence, strength parameters of materials in the excavation damaged zone are different and subjected to the deterioration as a result of damaged induced effects (Zareifard and Fahimifar, 2016). These parameters are $\sigma_c^{'}$, $\sigma_t^{'}$, $\tau_0^{'}$, $m^{'}$, $s^{'}$, $and a^{'}$, respectively, for compressive strength, tensile strength, shear strength, and Hoek-Brown constants of damaged rock mass. This strength parameters can be calculated using proper application of disturbance parameter and relationships proposed in Hoek et al. (2002). Also, parameters used as plastic potential parameters in the excavation damaged zone, $m_g^{'}$, $s_g^{'}$, $a_g^{'}$, $and \varphi^{'}$, may vary from those used in the plastic region (Zareifard and Fahimifar, 2016).

3. Development of stress-strain formulation

In this section, the required equations (including both preliminary basic equations and newly derived ones) to obtain the comprehensive, new ground reaction curve based on the newly defined medium are derived. First, radial and tangential stresses and strains around the tunnel should be calculated. It can be explained that radial stress on the $r = R_P$ (outer plastic zone) is equal to $\sigma_r = \sigma_R$. This point corresponds to the elastic-plastic boundary. Indeed, when the plastic zone is formed, the radial stress σ_R, acting on the elastic–plastic interface is equal to P_{ic}. Its value is independent of radius and the radius of plastic zone can be obtained during calculations. Also, radial stress at the inner plastic boundary (plastic-EDZ boundary) is then calculated using Runge-Kutta-

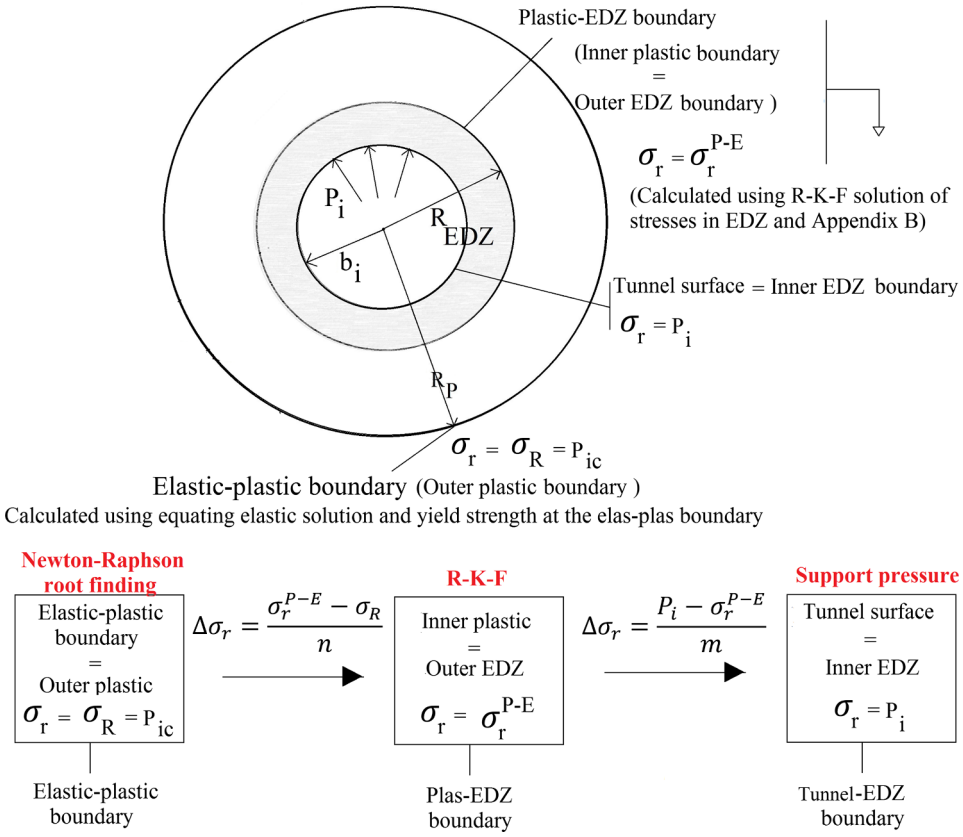

Fig. 2. Stresses at different regions.

Fehlberg solution of governing equilibrium equation of excavation damaged zone. This boundary is, also, called outer EDZ boundary. Tunnel's surface is the other problem's boundary (boundary between tunnel's surface and EDZ), which is called inner EDZ boundary. The value of radial stress at the inner EDZ boundary is equal to the tunnel's support pressure, . After solving the mentioned equations and calculating the described radial stresses at the boundaries, they will be assumed as a *priori* for the remaining solution domain. Fig. 2 better represents the described boundaries and solution steps. Noting that radial stresses on both inner and outer plastic zone boundaries are available as a *priori*, (Lee and Pietruszczak, 2008) calculated radial stress increment in the plastic zone for an elastic-plastic rock mass, $\Delta\sigma_r$, using a monotonical decrease from its value in $r = R_P$, $\sigma_r = \sigma_R$, to its value on the tunnel surface $r = b_i$, $\sigma_r = P_i$, where r represents distance from the tunnel center (Lee and Pietruszczak, 2008). In this paper, first, radial stress in the plastic-EDZ boundary, σ_r^{P-E}, is found using Runge-Kutta-Fehlberg numerical solution (Mathews and Fink, 2004) of governing differential equation, and then the region is divided into the plastic and excavation damaged zones, where the values of radial stresses in the elastic-plastic, σ_R, and the plastic-EDZ, σ_r^{P-E}, boundaries are available for the analysis of the plastic zone. Also, the values of radial stresses in the plastic-EDZ boundary, σ_r^{P-E}, and the tunnel surface, , are considered as a *priori* for the analysis of the excavation damaged zone.

As previously described, analyses in different regions are different regarding the material's strength parameters and behaviors. It is assumed that the plastic zone and excavation damaged zone are composed of n and m concentric annuluses, respectively. Fig. 3 shows i^{th} and j^{th} arbitrary elements in the plastic and excavation damaged zones, respectively. In this figure, i^{th} element is marked using $(i-1)^{th}$ and i^{th} circles with the normalized radiuses of ρ_{i-1} and ρ_i. Also, ρ'_{j-1} and ρ'_j respectively show the normalized radiuses of $(j-1)^{th}$ and j^{th} limiting circles in the EDZ.

Eqs. (22) and (23) present the normalized radiuses in the plastic and

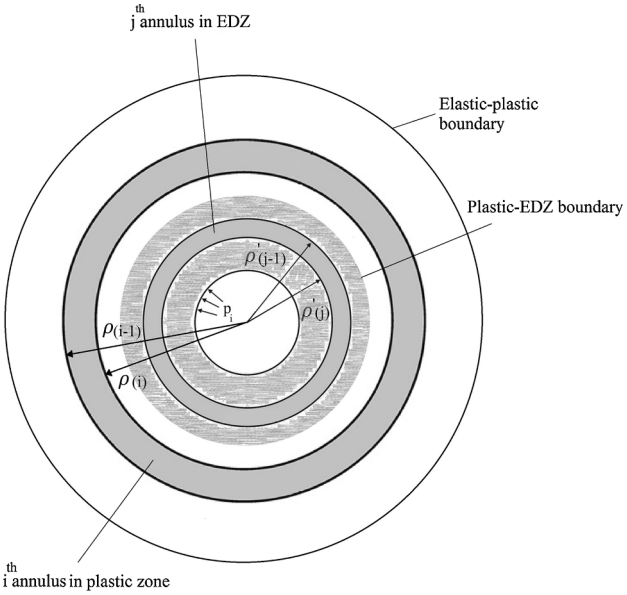

Fig. 3. Definition of arbitrary annuluses in plastic and EDZ regions around a circular tunnel in an elastic-plastic-EDZ rock mass.

damaged zones. As it can be inferred, $\rho_{(0)} = 1$ and $\rho_{(n)} = R_{EDZ}/R_P$, respectively, state outer and inner boundaries of the plastic zone. Similarly, $\rho'_{(0)} = 1$ and $\rho'_{(m)} = b_i/R_{EDZ}$ (a *priori*) are, respectively, outer, and inner normalized radiuses of EDZ boundaries.

$$\rho_{(i)} = \frac{r_{(i)}}{R_P} \tag{22}$$

$$\rho_{(j)}^{'} = \frac{r_{(j)}}{R_{EDZ}} \tag{23}$$

Thicknesses of both annuluses in the plastic and damaged zones are calculated in a way that the corresponding governing equilibrium equation is satisfied (this is further discussed in later sections). Hence, radial stress increments in both plastic and damaged zones are not constant. In order to solve the problem, radial and tangential stresses in the outer boundary of the plastic zone (Eqs. (24) and (25)) presented by Brown et al. (1983) are used as initial condition for the first solution step (stress-strain solution in the plastic zone). Also, using the results of n^{th} annulus as the initial condition for the second solution step (stress-strain solution in EDZ), total radial displacement around the tunnel can be calculated.

$$\begin{Bmatrix} \sigma_{r(0)} \\ \sigma_{\theta(0)} \end{Bmatrix} = \begin{Bmatrix} \sigma_R \\ 2\sigma_0 - \sigma_R \end{Bmatrix} \tag{24}$$

$$\begin{Bmatrix} \varepsilon_{r(0)} \\ \varepsilon_{\theta(0)} \end{Bmatrix} = \frac{1+\vartheta}{E} \begin{Bmatrix} \sigma_R - \sigma_0 \\ \sigma_0 - \sigma_R \end{Bmatrix} \tag{25}$$

where $\sigma_{r(0)}$, $\sigma_{\theta(0)}$, $\varepsilon_{r(0)}$ and $\varepsilon_{\theta(0)}$, respectively, present radial stress, tangential (hoop) stress, radial strain, and tangential strain in the elastic-plastic boundary. Also, E is Young's modulus and ϑ declares Poison's ratio of intact rock mass in the elastic zone (Brown et al., 1983).

3.1. Radial stress in the plastic-EDZ boundary

The equilibrium equation in the plastic zone for large numbers of constructing annulus is as follow (Lee and Pietruszczak, 2008):

$$\frac{d\sigma_r}{d\rho} + \frac{\sigma_r - \sigma_\theta}{\rho} = 0 \tag{26}$$

Regarding the weight of damaged zone, the material's governing equilibrium equation is different in EDZ. It is, also, different in different directions through the excavation damaged zone. It does affect the damaged rock masses' governing equilibrium equation in the tunnel's crown. It should be noted that the strength parameters deterioration in this zone will be the same for different directions. Hence, the present manuscript deals with the development of the proper solution method for the calculation of GRC in the crown and sidewalls of the tunnel. Derivation of the governing equilibrium equation in EDZ for the sidewall and crown directions is as follow:

In cylindrical coordinates (r, θ, z), the stress field around a tunnel (as depicted in Fig. 4) has to fulfill the following equilibrium equations (Eqs. (27) and (28)) for each element of the rock mass (Kolymbas, 2005):

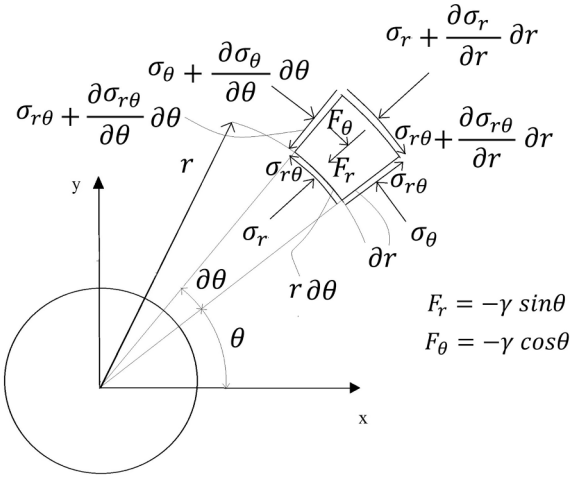

Fig. 4. Stresses and body forces in an arbitrary element around the tunnel.

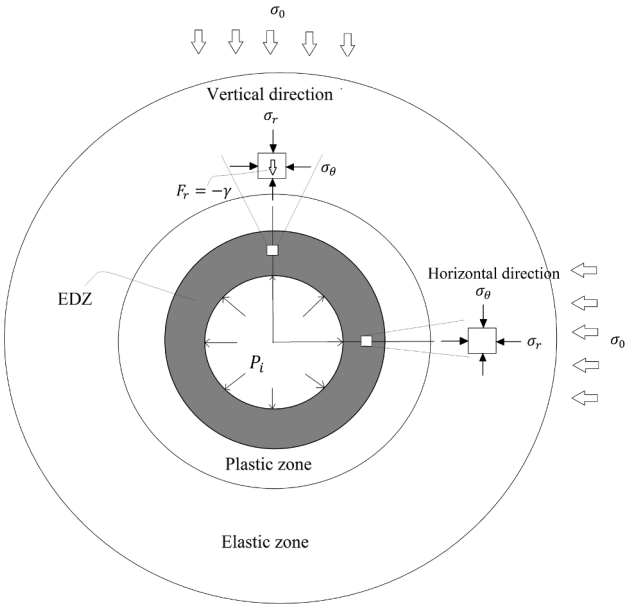

Fig. 5. Stresses and body forces in an arbitrary element in horizontal and vertical directions.

$$\frac{\partial \sigma_{rr}}{\partial r} + \frac{1}{r}\frac{\partial \sigma_{\theta r}}{\partial \theta} - \frac{\sigma_{\theta\theta} - \sigma_{rr}}{r} + F_r = 0 \tag{27}$$

$$\frac{\partial \sigma_{r\theta}}{\partial r} + \frac{1}{r}\frac{\partial \sigma_{\theta\theta}}{\partial \theta} + \frac{\sigma_{r\theta} + \sigma_{\theta r}}{r} + F_\theta = 0 \tag{28}$$

where σ_{rr}, $\sigma_{\theta\theta}$, $\sigma_{r\theta}$ and $\sigma_{\theta r}$ are stress components, while F_r and F_θ represent body forces.

Regarding the basic assumptions of the convergence-confinement method (hydrostatic stress field and a uniform internal support pressure), also, considering that this research proposes the solution for the tunnel's crown (in the vertical direction) and sidewalls (in the horizontal direction), the problem follows of assumptions considered in Zareifard and Fahimifar (2012), Fahimifar et al. (2014) and hence, the problem will be simplified into Fig. 5 for the horizontal and vertical directions. Hence, the term "$\frac{1}{r}\frac{\partial \sigma_{\theta r}}{\partial \theta}$" will be vanished and the equilibrium equation will be simplified into Eq. (29).

$$\frac{d\sigma_r}{dr} - \frac{\sigma_\theta - \sigma_r}{r} + F_r = 0 \tag{29}$$

where F_r is the radial term of the body force and depends on the gravitational load in EDZ with respect to the direction. Since $F_r = -\gamma \sin\theta$, the term of body force in the vertical direction will be "$-\gamma$", while it equals to zero at the horizontal direction. Hence, the equation of equilibrium in the damaged zone, will be as Eq. (30) for the vertical direction. The same method has, also, been used by Zareifard and Fahimifar (2012), Fahimifar et al. (2014) to develop the stress around the circular tunnel for the case of Hoek-Brown strength criterion and consideration of gravitational loads exerted to the shallow tunnels, where a strain softening, elastoplastic solution is presented. Regarding this equation and considering the normalized radius in EDZ, Eqs. (31) and (33), respectively, present damaged rock masses' governing equilibrium equations in the tunnel's crown and sidewalls.

$$\frac{d\sigma_r}{dr} + \frac{\sigma_r - \sigma_\theta}{r} - \gamma^{'} = 0 \tag{30}$$

$$\frac{d\sigma_r}{d\rho^{'}} = \frac{H^{'}(\sigma_r)}{\rho^{'}} + \gamma^{'} R_{EDZ} \tag{31}$$

$$H'(\sigma_r) = \frac{2(b'+1)}{(2+b')}\sigma_c'\left(m_b'\frac{\sigma_r}{\sigma_c'}+s'\right)^{a'} \tag{32}$$

$$\frac{d\sigma_r}{d\rho'} = \frac{H'(\sigma_r)}{\rho'} \tag{33}$$

where "*prime*" superscript denotes the excavation damaged zone's parameters. Also, γ' is the unit weight of damaged rock mass in EDZ. Regarding the nonlinearity of the developed differential equations, there is not any analytical solution to the problem. Hence, Eqs. (31) and (33) are solved using the fifth order Runge-Kutta-Fehlberg method considering initial value condition at the tunnel surface ($\sigma_r = P_i$ at $r = b_i$) (Mathews and Fink, 2004). And, σ_r^{P-E} in the plastic-EDZ boundary are calculated for the tunnel's crown and sidewalls.

3.1.1. Runge-Kutta-Fehlberg method to gain radial stress in the plastic-EDZ boundary

To solve Eqs. (31) and (33), the Runge-Kutta-Fehlberg solution method can be used. In this method, the first order ordinary nonlinear differential equation of damaged rock mass equilibrium is solved considering initial value condition $\sigma_r = P_i$ at $r_i = b_i(\rho_0' = b_i/R_{EDZ})$.

For an assumed equilibrium equation in the form of Eq. (31), function f is defined as shown in Eq. (35).

$$f(\rho', \sigma_r) = \frac{d\sigma_r}{d\rho'} = \frac{H'(\sigma_r)}{\rho'} + \gamma' R_{EDZ} \tag{34}$$

Fourth and fifth order approximations to the solution of the problem are, respectively, presented in Eqs. (35) and (36) (Mathews and Fink, 2004).

$$y_{k+1} = y_k + \frac{25}{216}k_1 + \frac{1408}{2565}k_3 + \frac{2197}{4101}k_4 - \frac{1}{5}k_5 \tag{35}$$

$$z_{k+1} = y_k + \frac{16}{135}k_1 + \frac{6656}{12825}k_3 + \frac{28561}{56430}k_4 - \frac{9}{50}k_5 + \frac{2}{55}k_6 \tag{36}$$

where k_i coefficients are calculated using following equations. Also, y_{k+1} and z_{k+1} are fourth order and fifth order approximation of the equilibrium equation in the plastic-EDZ boundary, respectively. Coefficients used to calculate k_i are presented in Table 2.

$$k_1 = hf(t_k, y_k) \tag{37}$$

$$k_i = hf\left(t_k + a_i h, y_k + \sum_{j=2}^{i} b_{(i)(j-1)}k_{j-1}\right) \quad \& \quad i \in (2, 6) \tag{38}$$

In these equations, t_k and y_k, respectively, represent ρ_j' and σ_r values in each of solution steps, and h defines the selected step size. The accuracy of the solution is acceptable when the following equation is satisfied (Mathews and Fink, 2004):

$$Tolerance = |z_{k+1} - y_{k+1}| \le Acceptable \quad Tol \tag{39}$$

where *Tol* is the pre-defined acceptable accuracy for prediction of σ_r^{P-E}.

Table 2
Coefficients used to calculate k_i of R-K-F solution.

i	a_i	$b_{(i)(j-1)}$				
		j = 2	j = 3	j = 4	j = 5	j = 6
2	$\frac{1}{4}$	$\frac{1}{4}$	–	–	–	–
3	$\frac{3}{8}$	$\frac{3}{32}$	$\frac{9}{32}$	–	–	–
4	$\frac{12}{13}$	$\frac{1932}{2197}$	$-\frac{7200}{2197}$	$\frac{7296}{2197}$	–	–
5	1	$\frac{439}{216}$	-8	$\frac{3680}{513}$	$-\frac{845}{4104}$	–
6	$\frac{1}{2}$	$-\frac{8}{27}$	2	$-\frac{3544}{2565}$	$\frac{1859}{4104}$	$-\frac{11}{40}$

Also, *Tolerance* parameter shows the value of tolerance calculated in each step size. In order to increase the accuracy of prediction and satisfy the controlling equation, Eq. (39), step size, h, can be reduced. The optimum step size can be found using multiplying s variable presented in Eq. (40) to the current h (Mathews and Fink, 2004).

$$s = 0.84 \times \left(\frac{h \times Tol}{|z_{k+1} - y_{k+1}|}\right)^{1/4} \tag{40}$$

The developed Fortran program to obtain the value of σ_r^{P-E} using a fifth order Runge-Kutta-Fehlberg step size control solution scheme (Mathews and Fink, 2004) is presented in "Supplementary material B".

(Park, 2014) applies the Cash-Karp version of the Runge-Kutta-Fehlberg (R-K-F) approach (Chapra and Canale, 2002) to solve their self-similarity equations in the plastic region (Park, 2014). Since it uses this method in the solution of stress-strains in the plastic region, it is subjected to a transition region, softening-residual boundary, where strength parameters are different in the two different zones and result in different governing equations. Hence, instable results are gained through their solution for Hoek-Brown criterion. In such cases, the classical Runge-Kutta method is applied to overcome this difficulty. In addition, not using a proper optimum adaptive step size may be another possible cause of the observed tolerances. Nevertheless, in this paper, the optimum adaptive step size control and original R-K-F method is used. In addition, the equation of equilibrium in the excavation damaged zone does not contain a transition zone and therefore results in accurate results.

3.2. Stress-strain relationships in the plastic zone

As described in the previous sections, the radial stress and the increments of radial stress in the plastic zone are calculated based on the initial conditions and the preliminary calculations of σ_R and σ_r^{P-E}. General calculations presented in this section are similar to those presented by Lee and Pietruszczak (2008). However, the used strength criterion (along with its corresponding input parameters), initial boundary conditions, also, the dilation and critical softening parameter calculations are different.

Radial stress through the plastic zone is obtained using the monotonic decrease of σ_R (in the elastic-plastic boundary) to the σ_r^{P-E} (in the plastic-EDZ boundary). Hence, radial stress increment is assumed to be obtained using Eq. (41).

$$\Delta\sigma_r = \frac{\sigma_r^{P-E} - \sigma_R}{n} \tag{41}$$

where $\Delta\sigma_r$ is the radial stress increment and n represents the number of annuluses in the plastic zone.

It should be noted that although the increment of radial stress is constant throughout the plastic zone, the thicknesses of annuluses are not the same. This is because the radius of each annulus is calculated in a way that the corresponding governing equilibrium equation is satisfied.

3.2.1. Stresses

Starting from the elastic-plastic boundary with the radial stress of σ_R, Eq. (42) is used to calculate the radial stress of each annulus in the plastic zone (Lee and Pietruszczak, 2008). Also, the corresponding tangential stress of each annulus and its increment can be found by applying Eq. (42) into Eq. (25) and Eq. (1) based on the simple calculations presented in Eqs. (43) and (44) (Lee and Pietruszczak, 2008).

$$\sigma_{r(i)} = \sigma_{r(i-1)} + \Delta\sigma_r \tag{42}$$

$$\sigma_{\theta(i)} = \sigma_{r(i)} + H(\sigma_{r(i)}, \gamma_{i-1}^p) \tag{43}$$

$$\Delta\sigma_{\theta(i)} = \sigma_{\theta(i)} - \sigma_{\theta(i-1)} \tag{44}$$

3.2.2. Strains

Elastic strain increments are calculated based on Hook's law using radial and tangential stress increments as below (Lee and Pietruszczak, 2008):

$$\begin{Bmatrix}\Delta\varepsilon^{e}_{r(i)}\\ \Delta\varepsilon^{e}_{\theta(i)}\end{Bmatrix}=\frac{1+\vartheta}{E}\begin{bmatrix}1-\vartheta & -\vartheta\\ -\vartheta & 1-\vartheta\end{bmatrix}\begin{Bmatrix}\Delta\sigma_{r(i)}\\ \Delta\sigma_{\theta(i)}\end{Bmatrix} \tag{45}$$

where E and ϑ are, respectively, Young's modulus and Poison's ratio of intact rock mass in the elastic zone. $\Delta\varepsilon^{e}_{r(i)}$ is the elastic radial strain increment, also, $\Delta\varepsilon^{e}_{\theta(i)}$ represents elastic tangential strain increment. To obtain radial and tangential strain in the plastic region, plastic parts of radial and tangential strains must be defined. First, using the governing equilibrium equation in the plastic zone, Eq. (26), the value of i^{th} normalized radius (starting from $\rho_{(0)}=R_P/R_P=1$) is approximated using Eq. (46), like the equation presented by Lee and Pietruszczak (2008).

$$\rho_{(i)}=\frac{2H(\bar{\sigma}_{r(i)},\gamma^{p}_{i-1})+\Delta\sigma_r}{2H(\bar{\sigma}_{r(i)},\gamma^{p}_{i-1})-\Delta\sigma_r}\rho_{(i-1)} \tag{46}$$

where $\bar{\sigma}_{r(i)}=(\sigma_{r(i)}+\sigma_{r(i-1)})/2$.

Then, following similar steps, the plastic tangential strain increment can be calculated using Eq. (47) (Lee and Pietruszczak, 2008).

$$\Delta\varepsilon^{p}_{\theta(i)}=\frac{-\frac{\Delta\varepsilon^{e}_{\theta(i)}}{\Delta\rho_{(i)}}-\frac{1+\vartheta}{E}\frac{H(\bar{\sigma}_{r(i)},\gamma^{p}_{i-1})}{\bar{\rho}_{(i)}}-\frac{1}{\bar{\rho}_{(i)}}(\varepsilon^{p}_{\theta(i-1)}-\varepsilon^{p}_{r(i-1)})}{\frac{1}{\Delta\rho_{(i)}}+\frac{1}{\bar{\rho}_{(i)}}(1+k_{(i-1)})} \tag{47}$$

where $\bar{\rho}_{(i)}=(\rho_{(i)}+\rho_{(i-1)})/2$. In this equation, $k_{(i-1)}$ can be defined regarding the different behaviors of potential function using each of Eqs. (14), (15), or (16). Then, $\Delta\varepsilon^{p}_{r(i)}$ is calculated using Eqs. (13) and (47). The equation for the development of strain softening parameter in plastic zone for different annulus radiuses is presented in Eq. (48) (Alejano et al., 2010; Lee and Pietruszczak, 2008; Park et al., 2008; Zareifard and Fahimifar, 2012).

$$\gamma^{p}_{(i)}=\gamma^{p}_{(i-1)}+(\Delta\varepsilon^{p}_{\theta(i)}-\Delta\varepsilon^{p}_{r(i)}) \tag{48}$$

Finally, total radial and tangential strain for an arbitrary annulus in the plastic zone is calculated using Eq. (49).

$$\begin{Bmatrix}\varepsilon_{r(i)}\\ \varepsilon_{\theta(i)}\end{Bmatrix}=\begin{Bmatrix}\varepsilon_{r(i-1)}\\ \varepsilon_{\theta(i-1)}\end{Bmatrix}+\begin{Bmatrix}\Delta\varepsilon^{e}_{r(i)}\\ \Delta\varepsilon^{e}_{\theta(i)}\end{Bmatrix}+\begin{Bmatrix}\Delta\varepsilon^{p}_{r(i)}\\ \Delta\varepsilon^{p}_{\theta(i)}\end{Bmatrix} \tag{49}$$

Also, the radius of the plastic region, r_P, can be calculated by repeating the described sequential approach for n times using the normalized radius of the last annulus in the plastic zone (Eq. (50)).

$$r_P=\frac{R_{EDZ}}{\rho_{(i=n)}} \tag{50}$$

3.3. Stress-strain relationships in EDZ

The strength parameters of rock mass in the excavation damaged zone changes. In fact, due to the blast- or excavation-induced effects, materials' strength parameters are weakened. Eqs. (51) and (52) show materials' governing strength criterion in the excavation damaged zone. In these relationships, superscript "*Prime*" represents the weakened strength parameters of rock mass in the damaged zone.

$$F(\sigma_\theta,\sigma_r)=\sigma_\theta-\sigma_r-H'(\sigma_r) \tag{51}$$

$$H'(\sigma_r)=\frac{2(b'+1)}{(2+b')}\sigma_c'\left(m_b'\frac{\sigma_r}{\sigma_c'}+s'\right)^{a'} \tag{52}$$

As previously described, the results of radial, $\sigma_{r(i=n)}=\sigma_r^{P-E}$, and tangential stresses, $\sigma_{\theta(i=n)}$, in the last annulus of the plastic zone, $(i=n)$, are considered as initial conditions for the excavation damaged zone, $\sigma_{r(j=0)}=\sigma_{r(i=n)}=\sigma_r^{P-E}$ and $\sigma_{\theta(j=0)}=\sigma_{\theta(i=n)}$. In these initial conditions, j represents the number of each of the annuluses in the EDZ. In this zone, starting from σ_r^{P-E}, radial stress monotonically decreases toward the value of internal support pressure, . The increment of radial stress in this zone is assumed to be calculated using Eq. (53). Similar to the plastic zone, thickness of radial stress in EDZ is not constant since the normalized radius in EDZ, $\rho'_{(j)}$, is computed in a way to satisfy the governing equilibrium equation. Also, the number of annuluses in EDZ is equal to m, which is sufficiently large to satisfy the desired accuracy of stress-strain predictions. After calculation of radial displacement in the plastic zone, in the excavation damaged zone, initial total strains will be equal to zero, $\varepsilon_{r(j=0)}=\varepsilon_{\theta(j=0)}=0$. And, the total radial displacement will be equal to the summation of the value of the radial displacement at the plastic-EDZ boundary and the occurred radial displacement in the excavation damaged zone. Other initial boundary conditions for excavation damaged zone are $\varepsilon_r^p=\varepsilon_\theta^p=\varepsilon_r^e=\varepsilon_\theta^e=\Delta\varepsilon_r^p=\Delta\varepsilon_\theta^p=\Delta\varepsilon_r^e=\Delta\varepsilon_\theta^e=0$ and $\rho'_{(j=0)}=1$.

$$\Delta\sigma_r=\frac{P_i-\sigma_r^{P-E}}{m} \tag{53}$$

In the excavation damaged zone, the weight of the damaged zone is taken into the consideration, and materials' governing equilibrium equations are different for different directions around the tunnel. Hence, in Eq. (53), the term σ_r^{P-E} is different for the tunnel's sidewall and crown, resulting in different $\Delta\sigma_r$ values for the tunnel's sidewall or crown.

3.3.1. Tunnel's sidewall

In the tunnel's sidewall direction, the unit weight of material will be zero in the governing equilibrium equation and hence, the general form of the equilibrium equation in the EDZ (in the tunnel's sidewall) is similar to that in the plastic region. But, the material's strength parameters in this zone are weakened and this is the main difference between governing equilibrium equations in the plastic region and EDZ in the sidewall direction. Another main difference between these two regions is the newly defined radius-dependent Young's modulus in EDZ, which changes the state of elastic and plastic radial and tangential strain increments. The governing equilibrium equation in this case is presented as Eq. (54).

$$\frac{d\sigma_r}{d\rho'}-\frac{H'(\sigma_r)}{\rho'}=0 \tag{54}$$

3.3.1.1. Stresses. Radial and tangential stresses of damaged rock mass in the tunnel's sidewall direction is calculated by applying the general form of Eqs. (42)–(44), where the term of $H(\sigma_{r(i)},\gamma^{p}_{i-1})$ in Eq. (43) is replaced by $H'(\sigma_r)$ and the term $\Delta\sigma_r$ in Eq. (42) must be calculated using Eq. (53). The new form of stress update is presented in Eqs. (55) and (56).

$$\sigma_{r(i)}=\sigma_{r(i-1)}+\frac{P_i-\sigma_r^{P-E}}{m} \tag{55}$$

$$\sigma_{\theta(i)}=\sigma_{r(i)}+H'(\sigma_r) \tag{56}$$

3.3.1.2. Strains. Radial and tangential elastic strain increments in EDZ in the sidewall direction are obtained by replacing Young's modulus in Eq. (45) with the new varying Young's modulus, $E'_{(j)}$ (presented in the following sections).

Then, the governing equilibrium equation, Eq. (54), is approximated for the j^{th} annulus as:

$$\frac{\sigma_{r(j)}-\sigma_{r(j-1)}}{\rho'_{(j)}-\rho'_{(j-1)}}-\frac{2H'(\bar{\sigma}_{r(j)})}{\rho'_{(j)}+\rho'_{(j-1)}}=0 \tag{57}$$

where $\bar{\sigma}_{r(j)}=(\sigma_{r(j)}+\sigma_{r(j-1)})/2$.

The normalized radius used for calculation of the plastic radial and

tangential strain increments in the sidewall direction of the tunnel can then be presented as following:

$$\rho_{(j)}^{'} = \frac{2H^{'}(\bar{\sigma}_{r(j)}) + \Delta\sigma_r}{2H^{'}(\bar{\sigma}_{r(j)}) - \Delta\sigma_r}\rho_{(j-1)}^{'} \tag{58}$$

The compatibility equation can be written as (Florence and Schwer, 1978):

$$\frac{d\varepsilon_\theta}{d\rho^{'}} + \frac{\varepsilon_\theta - \varepsilon_r}{\rho^{'}} = 0 \tag{59}$$

Hence, regarding the elastic and plastic portions of the radial and tangential strains, the governing strength criterion, Eq. (59), can be reformulated as Eq. (60).

$$\frac{d\varepsilon_\theta^p}{d\rho^{'}} + \frac{\varepsilon_\theta^p - \varepsilon_r^p}{\rho^{'}} = -\frac{d\varepsilon_\theta^e}{d\rho^{'}} - \frac{\varepsilon_\theta^e - \varepsilon_r^e}{\rho^{'}} = -\frac{d\varepsilon_\theta^e}{d\rho^{'}} - \frac{1+\vartheta}{E^{'}}\frac{H^{'}(\sigma_r)}{\rho^{'}} \tag{60}$$

Eq. (61) is then derived for $\Delta\varepsilon_\theta^p$ in EDZ (in the sidewall direction) based on the approximation of Eq. (60) with respect to $\rho^{'}$.

$$\Delta\varepsilon_{\theta(j)}^p = \frac{-\frac{\Delta\varepsilon_{\theta(j)}^e}{\Delta\rho_{(j)}^{'}} - \frac{1+\vartheta}{E_{(j)}^{'}}\frac{H^{'}(\bar{\sigma}_{r(j)})}{\bar{\rho}_{(j)}^{'}} - \frac{1}{\bar{\rho}_{(j)}^{'}}(\varepsilon_{\theta(j-1)}^p - \varepsilon_{r(j-1)}^p)}{\frac{1}{\Delta\rho_{(j)}^{'}} + \frac{1}{\bar{\rho}_{(j)}^{'}}(1 + k_{(j-1)}^{'})} \tag{61}$$

where $k^{'}$ represents the relationship between radial and tangential strain increments in EDZ in the sidewalls and is calculated using one of Eq. (14) ($k^{'} = k^p(\gamma^p = 0)$ for different $\Psi^{'}$ values in each of the annuluses in EDZ), (15), or (16). It should **be** noted that to obtain $k^{'}$, the parameters associated with the potential function in the damaged zone - $m_g^{'}$, $s_g^{'}$, $a_g^{'}$ and $\varphi^{'}$ - and $\sigma_c^{'}$ must be used. This approach can be applied where sufficient data is available regarding the plastic potential function in EDZ. But, in cases where there is no access to required data associated with the variation of the plastic potential function's parameters in EDZ, these parameters may be assumed constant and equal to the last value of their corresponding parameters in the plastic zone. In Eq. (61), $\bar{\rho}_{(j)} = (\rho_{(j)} + \rho_{(j-1)})/2$. Also, corresponding $\Delta\varepsilon_{\theta(j)}^p$ is calculated using Eq. (62).

$$\Delta\varepsilon_{r(j)}^p = -k_{(j-1)}^{'}\Delta\varepsilon_{\theta(j)}^p \tag{62}$$

Then, similar to Eq. (49), total radial and tangential strains are calculated using the summation of their cumulative previous values with their corresponding elastic and plastic increments (Eq. (63)).

$$\begin{Bmatrix}\varepsilon_{r(j)}\\ \varepsilon_{\theta(j)}\end{Bmatrix} = \begin{Bmatrix}\varepsilon_{r(j-1)}\\ \varepsilon_{\theta(j-1)}\end{Bmatrix} + \begin{Bmatrix}\Delta\varepsilon_{r(j)}^e\\ \Delta\varepsilon_{\theta(j)}^e\end{Bmatrix} + \begin{Bmatrix}\Delta\varepsilon_{r(j)}^p\\ \Delta\varepsilon_{\theta(j)}^p\end{Bmatrix} \tag{63}$$

Considering the relation $\varepsilon_\theta = u/r$, the normalized displacement, $U_{(j)}$, can be achieved using Eq. (64).

$$U_{(j)} = U_{(i=n)} + \varepsilon_{\theta(j)}\rho_j^{'} \tag{64}$$

Hence, the radial displacement at any location around the tunnel can be attained using Eq. (65).

$$u_{(j)} = u_{(i=n)} + (\varepsilon_{\theta(j)}\rho_j^{'}) \times R_{EDZ} \tag{65}$$

Ground reaction curve for the tunnel's sidewall can then be derived using $u_{(j)} - P_i$ relationship.

3.3.2. Tunnel's crown

As described, the weight of the damaged zone will affect the equilibrium equation in the tunnel's crown and Eq. (26) will be the equation of equilibrium in the tunnel's crown in the excavation damaged zone.

Radial stress in different locations in the excavation damaged zone can be computed using R-K-F solution of Eq. (31) as derived in previous sections. Also, this equation is used here to incrementally calculate both stresses and strains around the tunnel. The procedure is similar to the one described for the tunnel's sidewall. But, regarding the different governing equilibrium equation, the equations for the normalized radius will be different. Hence, different stress and strains will be gained for the tunnel's crown.

In this case, the governing equilibrium equation for the j^{th} annulus in the excavation damaged zone can be approximated as:

$$\frac{\sigma_{r(j)} - \sigma_{r(j-1)}}{\rho_{(j)}^{'} - \rho_{(j-1)}^{'}} - \frac{2H^{'}(\bar{\sigma}_{r(j)})}{\rho_{(j)}^{'} + \rho_{(j-1)}^{'}} = \gamma^{'}R_{EDZ} \tag{66}$$

Solving Eq. (66) for $\rho_{(j)}^{'}$ with finite difference approximation, the following expression is obtained:

$$\rho_{(j)}^{'} = \frac{1}{2\gamma^{'}R_{EDZ}}(\Delta\sigma_r - 2H^{'}(\bar{\sigma}_{r(j)}) + \sqrt{(2H^{'}(\bar{\sigma}_{r(j)}) - \Delta\sigma_r)^2 + 4\gamma^{'}R_{EDZ}(\gamma^{'}R_{EDZ}\rho_{(j-1)}^{'\ 2} + (2H^{'}(\bar{\sigma}_{r(j)}) + \Delta\sigma_r)\rho_{(j-1)}^{'})}) \tag{67}$$

Following similar steps as in the equations and steps for the tunnel's sidewall in EDZ, $\Delta\varepsilon_{\theta(j)}^p$, $\Delta\varepsilon_{r(j)}^p$, $\varepsilon_{r(j)}$, $\varepsilon_{\theta(j)}$, U_i, and u_i are derived. Then, the ground reaction curve (in the tunnel's crown) of rock mass around the tunnel can be depicted plotting different $P_i - u_i$.

4. Proposed algorithm for calculation of the new comprehensive GRC

In this section, using a schematic algorithm, sequential steps required to obtain GRC is presented. To do this, first, calculation of P_{ic} and the process of defining varying Young's modulus through the damaged zone is described and then the proposed algorithm is presented.

4.1. Derivation of critical support pressure

Critical support pressure demonstrates the supporting pressure, which controls the formation of the plastic zone. In cases where internal support pressure is less than its critical value, $P_{ic} = \sigma_R$ (radial stress in the elastic-plastic boundary), the plastic zone constitutes. It can be numerically obtained by applying the Newton-Raphson root finding method to the following nonlinear equation:

$$2(\sigma_0 - P_{ic}) = Y_p(m_p\frac{P_{ic}}{\sigma_{cp}} + s_p)^{a_p} = H_p \tag{68}$$

where p subscript denotes peak parameters. This equation uses two approaches to define differences between radial and tangential stresses in the elastic-plastic boundary, and equaling these two obtained terms (based on elasticity relationships and the values of stresses attained from rock strength criterion). The simple Newton-Raphson root finding Fortran code used to find P_{ic} is presented in "Supplementary material A". To better illustrate the calculations, Eq. (69) shows the gained relationship for P_{ic} using one Newton-Raphson iteration. In this solution, an initial guess for P_{ic} is calculated using peak strength parameters for corresponding intact rock (initial guess corresponds to the radial stress at the elastic-plastic boundary and hence satisfies the strength criterion for intact rock, $a_p = 0.5$).

$$P_{ic} = \left(\frac{Y_pA}{2} + \sigma_0\right) - \frac{Y_pA + Y_p\left[\frac{m_p}{\sigma_{cp}}\left(\frac{Y_pA}{2} + \sigma_0\right) + s_p\right]^{a_p}}{2 + \frac{Y_pa_pm_p}{\sigma_{cp}}\left[\frac{m_p}{\sigma_{cp}}\left(\frac{Y_pA}{2} + \sigma_0\right) + s_p\right]^{a_p-1}} \tag{69}$$

where the parameter A is equal to $\left[\frac{m_p}{4} - \sqrt{\left(m_p\frac{\sigma_0}{\sigma_{cp}} + \frac{m_p^2}{16} + s_p\right)}\right]$.

4.2. Young's modulus in EDZ

In spite of the assumption of a constant Young's modulus for the elastic and plastic regions, according to the (Saiang, 2008a), Young's modulus of damaged rock masses is not constant. Young's modulus as an index for quantifying a material's stiffness in EDZ, plays an

important role in the calculation of stresses and strains around the tunnel (Saiang, 2008a). As it proposes, Young's modulus of rock materials on the tunnel surface is assumed to be calculated using the equation proposed by Hoek and Diederichs (2006) (Eq. (70)) and considering the relevant disturbance factor, D.

$$E_m^{'} = 100000\left(\frac{1-\frac{D^{'}}{2}}{1+e^{\frac{75+25D^{'}-GSI^{'}}{11}}}\right) \tag{70}$$

where $D^{'}$ is the disturbance factor in the generalized form of the Hoek-Brown criterion, and GSI represents residual geological strength index.

Also, Young's modulus of rock mass in the plastic-EDZ boundary can be calculated by using a zero value for $D^{'}$ in Eq. (70) (Saiang, 2008a). Young's modulus through different radiuses of damaged rock masses in EDZ is calculated using Eq. (71), considering linear interpolation between the values of Young's modulus at the tunnel surface and the plastic-EDZ boundary (Saiang, 2008a).

$$E_{(j)}^{'} = E_0^{'} + \frac{E_m^{'} - E_0^{'}}{R_{EDZ}}[(\rho_{(j)}^{'} \times R_{EDZ}) - b] \tag{71}$$

where $E_j^{'}$ is Young's modulus of j^{th} annulus in the excavation damaged zone. Also, $E_m^{'}$ and $E_0^{'}$ are Young's modulus on the tunnel's surface, (with a relevant D value regarding the degree of disturbance exerted on the tunnel), and the plastic-EDZ boundary, ($D = 0$), respectively. It should be clarified that the superscript "," denotes that the corresponding parameter belongs to the excavation damaged zone and it is not referring to a different parameter. Indeed, according to Saiang (2008a), the modulus of the damaged zone calculated using Eq. (70) is occurred at the tunnel boundary and then varied linearly to the boundary of undamaged rock. In this boundary, D can be obtained using general recommendations proposed by Hoek et al. (2002) and Hoek (2012). Also, in Hoek (2012), it is emphasized that the blast damage factor D should not be applied to the entire rock mass surrounding the excavation and the damage factor D should only be applied to the actual zone of damaged. This is another proof for the fact that consideration of the excavation damaged zone enhances the accuracy of the modeling of the problem. Outside of the BIDZ the rock mass is considered undamaged and therefore $D = 0$ (i.e. no disturbance). It is noteworthy that in the cases that the formation of a damaged zone is neglected, in practice, the disturbance/damage factor is generally extended to the whole problem domain. Nevertheless, the described scheme adopted by Saiang (2008a) is proposed for the consideration of the damage factor in the problems, which consider the formation of such damaged zones.

The following algorithm (shown in Fig. 6) is used to develop a FORTRAN code to analyze the ground reaction curve of circular tunnels in an elastic-plastic-EDZ rock mass, which accounts for strain softening in the plastic region and obeys Unified strength criterion.

Also, detailed steps of different sections of the algorithm (presented in Fig. 6) along with the applied relationships to model GRCs are presented in "Supplementary material C".

5. Verification and comparison

To investigate the validity of the proposed algorithm, the results of field measurements of displacements occurred at the crown of Hanlingjie tunnel in Hunan, China at a depth of 146 m is used. Tunnel's section along with the geology conditions of the tunnel's site is presented in Fig. 7. The tunnel's support is composed of a sprayed concrete (with the thickness of 25 cm) and a lining of concrete layer with a width of 45 cm. Young's modulus, Poisson's ratio, compressive strength and the thickness of sprayed and lining concrete layers are illustrated in Fig. 7. Table 3 shows strength and other required parameters of the surrounding rock mass (Zou et al., 2017). Also, since the required date for the damaged zone is not presented, it is characterized with caution. Indeed, using all the applicable range for the parameters with uncertainties, the whole possible range is covered and the results are discussed. Based on the available data, the required data for characterizing EDZ can be presented as following: $m^{'} = 0.428$, $s^{'} = 0.0000395$, $a^{'} = 0.527$. These parameters are calculated using the back calculation of peak strength parameters resulting in $GSI_p = 41.88$ and $m_i = 17.7736$ and using Eq. (21) for $GSI^{'} = 27$ and $D^{'} = 0.6$ (value of disturbance factor for mechanical excavation in the damaged zone).

Some of the parameters of the damaged zone used for modeling purposes are as following: $\Psi^{'} = \Psi_r$, $\vartheta^{'} = \vartheta_r$ and $\gamma_{ave}^{'} = 28.65kN/m^3$ (based on the standard range of $\gamma^{'}$ for the Breccia rock mass, $(28.6 - 28.7)kN/m^3$).

As explained in the manuscript, some of the parameters required to characterize the proposed algorithm for the validation case are presented in Fig. 7 and Table 3 (as originally presented in Zou et al. (2017)). Other remaining parameters are calculated using the proper application of the available equations based on the basic strength parameters of the studied case. R_{EDZ} and b are the only remaining parameters, which their values are not presented.

The following descriptions illustrate the principles to define these two parameters:

Damaged zone around the tunnels are formed as a consequence of mechanical excavation or blasting operations. There are several methods to characterize the damaged zone and to predict/calculate the radius of the excavation induced/blast induced damaged zone. Among them, observation and classical method of Anläggnings AMA 98 (1999), which is developed based on the explosive type, charge diameter and charge concentration, also, scaling law proposed by Holmberg and Persson (1980), damping law proposed by Hustrulid et al. (1992), the quantified values using the (García-Bastante et al., 2012) method based on Langefor's theory of blast calculation or the results of experimental and field investigations of Saiang (2008b) can be effectively applied. Reports presented for the blast-induced damage investigations on the *SVEBEFO* project are other key resources for characterizing this zone (Andersson, 1992; Nyberg et al., 2000a, 2000b; Olsson and Bergqvist, 1993, 1995, 1997; Olsson et al., 2002; Olsson and Ouchterlony, 2003; Olsson et al., 2004).

Applying one of the described methods, the value of R_{EDZ} required for the characterization of the damaged zone in the proposed solution can be obtained. Also, according to the described methods and the results presented in González-Cao et al. (2013), the practical lower and upper bonds for the thickness of R_{EDZ} is $(1 - 2)m$.

Since the required information for the calculation of R_{EDZ} in the Hanlingjie tunnel (e.g. crack length, etc.) has not been presented, both lower and upper bonds of R_{EDZ} are investigated ($R_{EDZ} = 6.5\ m\ \ and\ \ 7.5\ m$, respectively, corresponding to the thickness of $1m$ and $2m$ for the damaged zone.

In addition, parameter b varies between 0 and 1. Hence, as its accurate value has not been experimentally measured in the original Zou et al. (2017), to comprehensively study the whole possible range for the variation of b, three different b values are investigated ($b = 0, 0.5\ \ and\ \ 1$). This allows the consideration of all the possible combinations for the variation of $R_{EDZ}\ \ and\ \ b$.

Results of field measurements along with the results of proposed algorithm (for both upper and lower bounds of the radius of the damaged zone, also, minimum, average and maximum b values) are presented in Fig. 8. As shown, all the R_{EDZ} and b values (in the range between upper and lower bonds) used to develop the GRC lead to acceptable pressure-displacement data pairs compatible to the field measurements in both measured displacements. The acceptable difference between the measured and calculated values shows the validity of the proposed algorithm in the development of GRC of circular tunnels in the strain softening, elastic-plastic-EDZ rock mass. It should be noted that the consideration of $R_{EDZ} = 7.5m$ and $b = 0.5$ results in the best

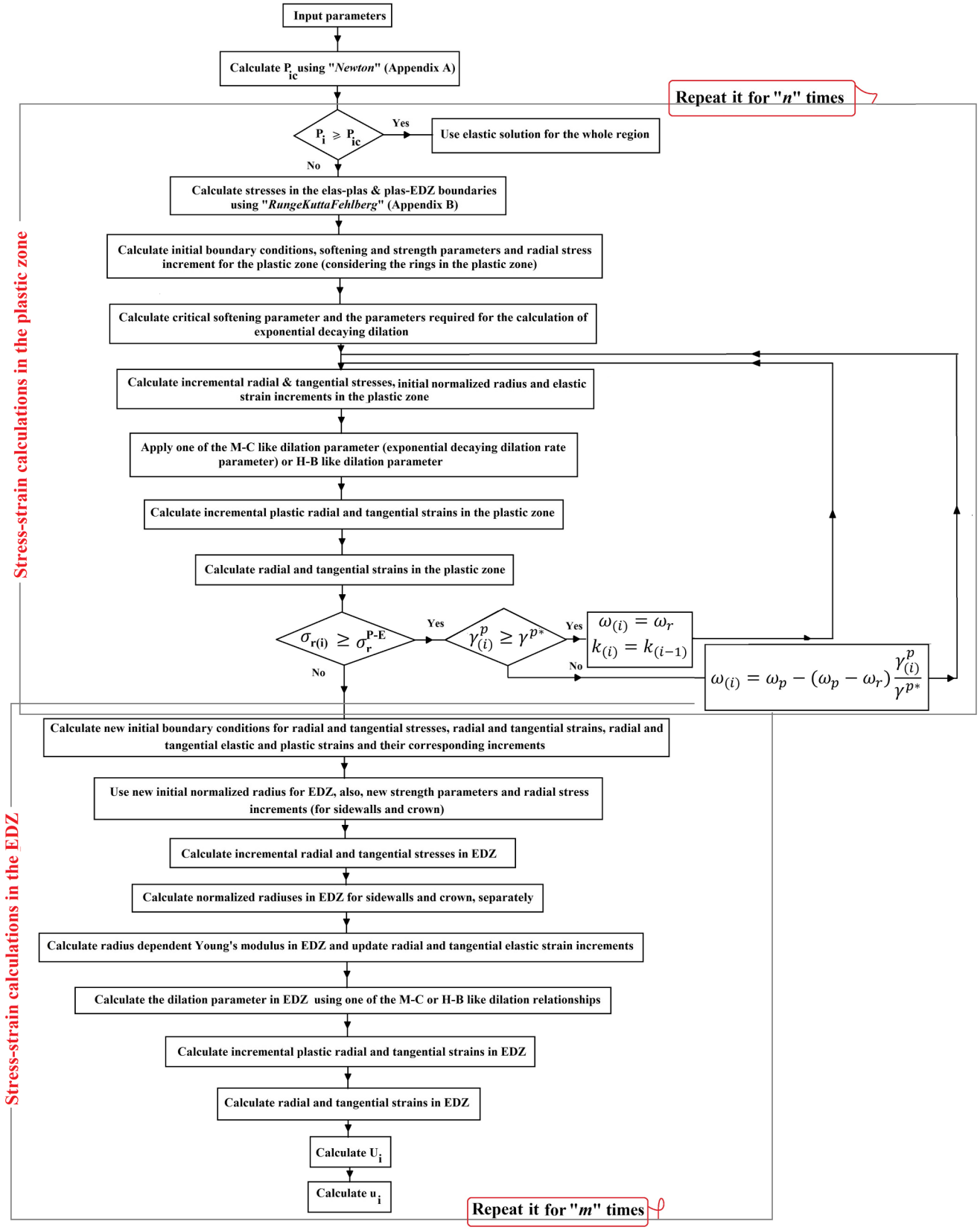

Fig. 6. Proposed algorithm for calculation of the new comprehensive GRC.

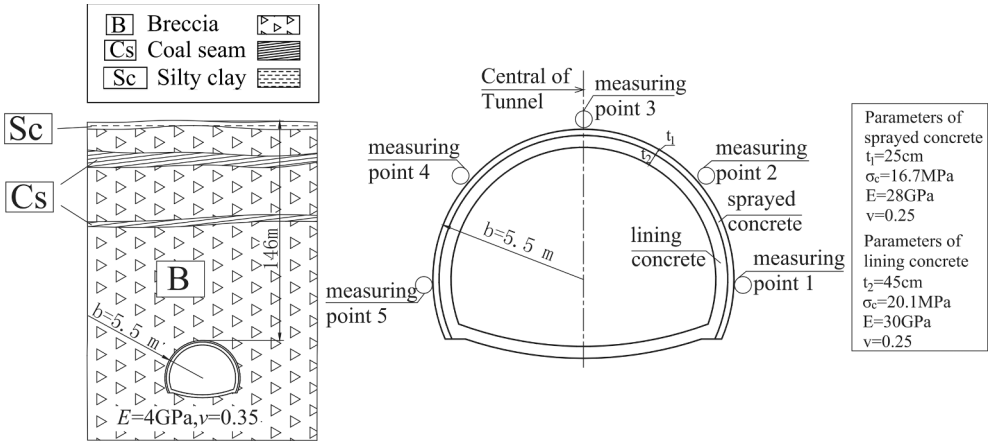

Fig. 7. Cross section and the site geology of Hanlingjie tunnel (Zou et al., 2017).

Table 3
Geometric and material properties of Hanlingjie tunnel's surrounding rock mass (Zou et al., 2017).

Parameter	Value
E_i	4 GPa
ϑ_i	0.35
σ_0	4.8 MPa
σ_{cp}	10 MPa
σ_{cr}	6 MPa
m_p	2.23
s_p	0.0013
a_p	0.51
m_r	0.86
s_r	0.0002
a_r	0.52
Ψ_p	12°
Ψ_r	5°
γ^{p*}	0.008

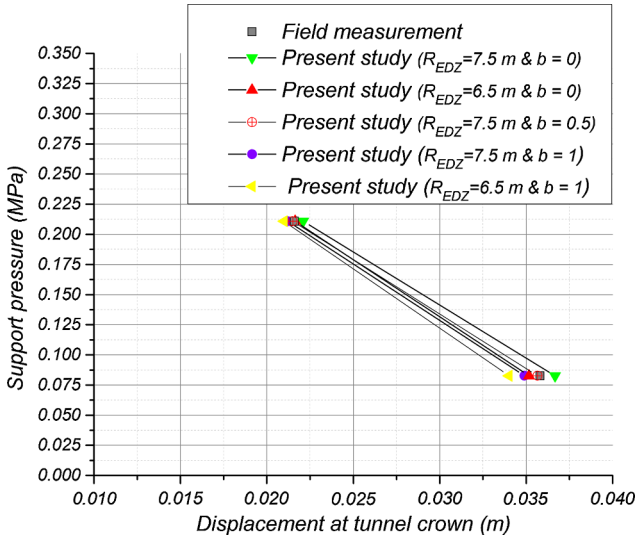

Fig. 8. Verification of the results of the proposed algorithm with the field measurements data.

fitness between the calculated and field monitoring data. This can be a proof for the positive effects of the proper consideration of these parameters in the development of GRC.

To investigate the comprehensiveness of the proposed algorithm in the prediction of ground reaction curve, first, three simplified cases are considered as comparison examples. Next, taking the new features of the proposed algorithm into the consideration, discrepancies between the available solutions and the proposed algorithm is further discussed. In the first section, the algorithm is simplified to the special cases (ignoring new features, which are not modeled in the literature) and the results of the proposed algorithm is compared to the cases with available solutions. Accuracy of the proposed algorithm can be examined through matching the results of the new algorithm with those available in the literature. Also, since the previous solutions partially treated with one of the described problem's complexities, well-validating the proposed algorithm with all the comparing examples will show its applicability in the comprehensive GRC modeling. Next, detailed discussions on the possible discrepancies are shown through applying new features to one of the available cases. As the first case of the first section, Section 5.1.1 considers a circular tunnel in an elastic-plastic rock mass case originally solved by Lee and Pietruszczak (2008) for a strain softening case. In this example, as shown in Table 1, no excavation damaged zone exists and eliminating that consideration, the proposed algorithm yields the same result as obtained by Lee and Pietruszczak (2008). This solution shows the accuracy of the user-coding process. Since the problem of a circular tunnel in the elastic-plastic, strain softening rock mass was also solved using a self-similar solution by Alonso et al. (2003), this example is also considered and the results of the proposed algorithm are compared to their self-similar solution. Second case, which deals with the consideration of variable post-peak dilatancy, presents the application of the exponential decaying post-peak dilation parameter originally proposed by Alejano and Alonso (2005) and Alejano et al. (2009). Since original models are only applied to the Mohr-Coulomb strength criterion, the studied case of Ketabian and Molladavoodi (2015), which uses the variable non-linear post-peak dilation parameter of Alejano and Alonso (2005) and Hoek-Brown strength criterion, is used. In this example, formation of an EDZ around the tunnel is not considered, and hence, the corresponding EDZ formulations are not used for comparison purposes (the problem is simplified to GRC development for the strain softening elastic-plastic rock mass with the variable post peak dilatancy). As described, it implements the variable dilatancy models into the newly developed iterative

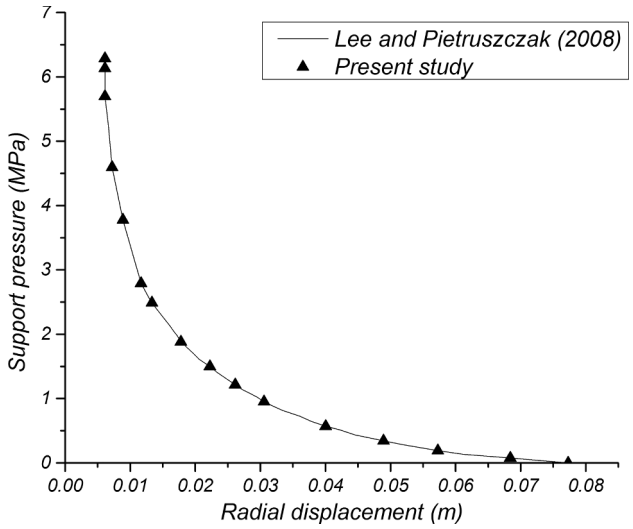

Fig. 9. Comparison with the ground reaction curve of Lee and Pietruszczak (2008); case $a_p = a_r = 0.5$.

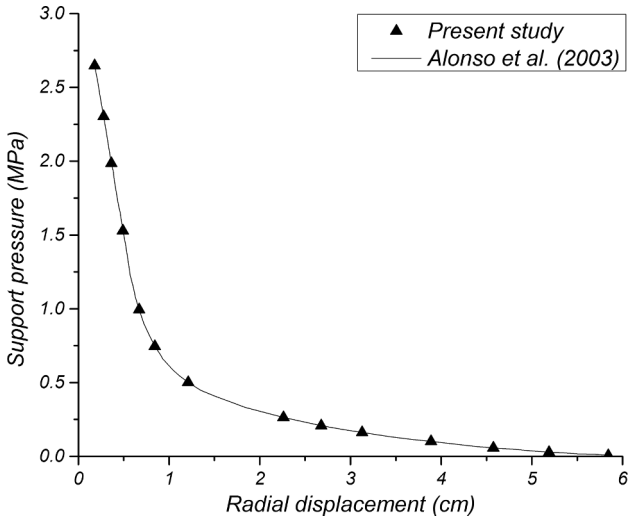

Fig. 10. Comparison with the ground reaction curve of Alonso et al. (2003).

solution and compares the results with the obtained results available in the literature, and these results are in agreement. As the third comparing case, the problem solved by Zareifard and Fahimifar (2016), the excavation damaged zone is modeled through assigning new strength parameters to EDZ (calculated using a Hoek-Brown D factor). Weight of EDZ, variation of Young's modulus in this zone, exponential decaying dilation parameter and strain softening in the plastic zone are not considered; as in two previous cases, the proposed algorithm is simplified to the conditions and assumptions of the example. The proposed algorithm is used to obtain GRC, radial displacement, radial stress, and tangential stress, and to compare them with those available from the simplified cases.

5.1. Elastic-plastic rock mass case considering strain softening

5.1.1. Comparison with (Lee and Pietruszczak, 2008)

In the problem solved by Lee and Pietruszczak (2008), a circular tunnel in an elastic-plastic rock mass with the following parameters is assumed. In this model, since the studied material is a medium rock mass, the effect of strain softening in the plastic zone has also been considered. Since it does not model the excavation damaged zone, step 4 of "Supplementary material C" in the proposed algorithm will be omitted and the solution will be only conducted for the plastic zone replacing σ_r^{P-E} with as the target radial stress. Also, the algorithm will be simplified to the first 16 steps (Supplementary material C) without variation of dilatancy (exponential decaying dilation parameter is not modeled) and drop modulus. Moreover, regarding the available material's strength parameters, effect of intermediate principle stress, b parameter, is not considered, and a Hoek-Brown strength criterion is used to develop the solution. The parameters used are: $b_i = 3m$, $\vartheta = 0.25$, $E = 5700\ MPa$, $\sigma_0 = 15\ MPa$, $\sigma_{cp} = 30\ MPa$, $\sigma_{cr} = 25\ MPa$, $m_p = 2$, $m_r = 0.6$, $s_p = 4e-3$, $s_r = 2e-3$, $a_p = a_r = 0.5$, $\Psi_p = 15^{\circ}$, $\Psi_r = 5^{\circ}$, $\gamma^{p*} = 0.01$ and $P_{ic} = 5.7027\ MPa$.

Fig. 9 presents the results of Lee and Pietruszczak (2008) along with those obtained from the proposed, new user-coded algorithm. Regarding the explained simplifications, the results are the same and as it can be seen, those results conform well to those obtained from the proposed algorithm.

5.1.2. Comparison with Alonso et al. (2003)

Similar to the example of Lee and Pietruszczak (2008), Alonso et al. (2003) considered a circular opening in an elastic-plastic rock mass experiencing the strain softening in the plastic zone. Hoek-Brown strength criterion with $a_p = a_r = 0.5$ was considered and compared to the proposed algorithm, effects of intermediate principle stress, exponential decaying dilation parameter, formation of EDZ (variation of Young's modulus in EDZ and deterioration of materials' strength parameters) are ignored. They used a self-similar solution to analyze their problem. Other used materials' and tunnel's parameters are as follows:

$b_i = 3m$, $\vartheta = 0.25$, $G = 552\ MPa$, $\sigma_0 = 3.31\ MPa$, $\sigma_c = 27.6\ MPa$, $m_p = 0.5$, $m_r = 0.1$, $s_p = 1e-3$, $s_r = 5e-4$, $\Psi_p = 15^{\circ}$, $\Psi_r = 5^{\circ}$, $\gamma^{p*} = 0.0125$ and $P_{ic} = 1.2159\ MPa$.

To compare results of the proposed algorithm with the self-similar solution of the example of Alonso et al. (2003), some simplifications (steps 4 and 16.9 is ignored, steps 17–19.21 are omitted and instead of

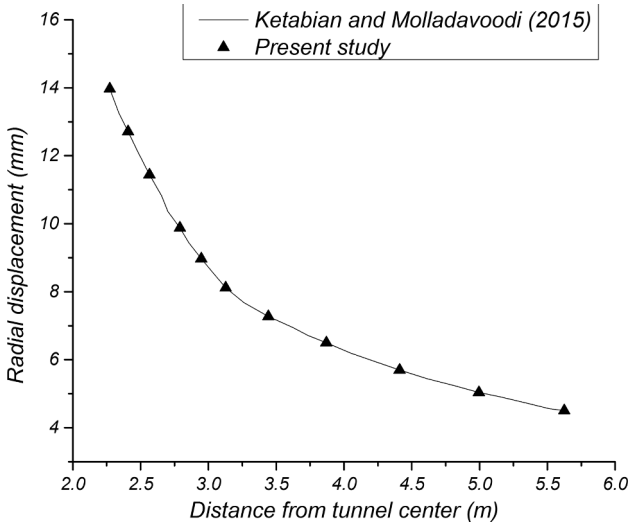

Fig. 11. Comparison with radial displacements of Ketabian and Molladavoodi (2015).

materials' strength parameters associated with the Unified strength criterion, Hoek-Brown strength parameters are used) are made to the proposed algorithm and the obtained results are presented in Fig. 10. As shown, results of the proposed algorithm are in a very close agreement with those presented in Alonso et al. (2003).

5.2. Strain softening rock mass case considering exponential decaying post-peak dilation parameter

In this example, the capability of the proposed method in modeling variable post-peak dilation coefficient is shown through modeling a simplified case (a case previously studied by Ketabian and Molladavoodi (2015)), in which the formation of damaged zone is not taken into account. Also, ignoring the effect of intermediate stresses, Hoek-Brown strength criterion is considered. Hence, the proposed algorithm will be simplified and step 4 (Supplementary material C) will be omitted. In this case, radial stress monotonically decreases from σ_R to reach . The first 16 steps of "Supplementary material C" are considered and radial displacements are obtained for different internal support pressures. Coefficient of dilation exponentially decreases from its peak value in the elastic-plastic boundary and is calculated using Eq. (14). The used input parameters are as following: $b_i = 2.25m$, $E = 6.5GPa$, $\vartheta = 0.25$, $\sigma_0 = 15.3MPa$, $P_i = 0$, $\sigma_C = 60MPa$, $m_i = 19$ and GSI_{peak} =50. As seen in Fig. 11, the obtained GRC is accurately identical to the results obtained by Ketabian and Molladavoodi (2015).

5.3. Elastic-perfect-plastic behavior of a rock mass case considering EDZ

The other example used to assess the performance of the proposed algorithm is a model developed by Zareifard and Fahimifar (2016). It should be noted that this example is referred as the case of a tunnel in a soft elastic-perfectly plastic rock mass (Zareifard and Fahimifar, 2016). Nevertheless, regarding the value of GSI, 50, it should be treated as a medium rock mass with a strain softening behavior. In this section, in order to compare the results of the original problem with the proposed algorithm, the softening behavior is ignored (as the original case is solved using an elastic- perfectly plastic behavior assumption). Next and in the future sections, this problem is re-solved using the proper strain-softening behavior and the results are compared.

In the model of Zareifard and Fahimifar (2016), the formation of EDZ is modeled by defining new strength parameters for EDZ. But, the weight of damaged rock in this zone, also, the variation of Young's modulus are not considered, and the proposed algorithm is then simplified. Also, in this simplified model, the effect of intermediate principle stress, exponential decaying dilation parameter and softening (as previously mentioned) is not considered. Section 4 of the proposed algorithm (Supplementary material C) is only used to solve Eq. (33) for all the tunnel's directions. Section 19.6.1 (Supplementary material C) of the proposed algorithm is used for both sidewall and crown directions (Section 19.6.2 is omitted). It only uses a constant value for Young's modulus in EDZ (Sections 19.8–19.10 are deleted). Also, the solved model does not consider strain softening in the plastic zone. Hence, $\omega_p = \omega_r$. In addition, variation of dilatancy is not considered in their modeling. The parameters used to solve the problem are as follows:

Material parameters in the plastic zone:

$\sigma_C = 30\ \ MPa$, $m_p = m_r = 1.7$, $s_p = s_r = 0.0039$, $GSI = 50$,

$E = 5500\ \ MPa$, $\Psi = 0$, $D = 0$

Material parameters in EDZ:

$E^{'} = 3800\ \ MPa$, $m^{'} = 0.8$, $s^{'} = 0.001$, $\sigma_c^{'} = 30\ \ MPa$, $\Psi^{'} = 0$ and $D = 0.6$

Other parameters used are $b_i = 5m$, $m_{intact} = 10$, $\vartheta = 0.25$, $\sigma_0 = 30MPa$, $P_i = 5MPa$. As can be seen, k, representing the relationship between radial and tangential plastic strain increments, is assumed to be constant for all the rings in both plastic zone and EDZ. Fig. 12, shows radial displacement, radial stress, and tangential stress around the tunnel versus distance from the tunnel's center for both the present study and Zareifard and Fahimifar (2016). As can be seen, the results gained from the new method accurately correlate with the simplified analytical solution of Zareifard and Fahimifar (2016). The accuracy of the obtained results shows that the proposed algorithm can comprehensively model different behaviors and situations, and that it can be efficiently used to model ground reaction curve of tunnels excavated in rock masses with complicated behaviors.

5.4. Effects of new features

To show effects of new features of the proposed algorithm, the problem originally solved by Zareifard and Fahimifar (2016), which separately presents the material parameters in the plastic and excavation damaged zones is considered. Then, effects of considering each of the new features of the proposed algorithm are investigated in separate sections. In the first section, intermediate principle stress is taken into the consideration through modeling the b parameter available in the USC (for different b values) and the results are compared to the original problem (which is solved based on Hoek-Brown criterion). Second section deals with effects of the weight of the damaged rock mass and compares the obtained GRCs for the cases that there is no weight effect to the case of applying the weight of the rock mass in the EDZ into the problem. Also, effects of existence of a softening zone, as well as an exponential decaying dilation behavior are examined in the third section. It should be noted that the following sections present the GRC of tunnels in the crown direction.

This section better presents the effectiveness and the importance of consideration of new features of the proposed algorithm in the modeling of ground reaction curve of rock masses.

5.4.1. Effect of the intermediate principle stress

The parameter b represents the effect of intermediate principle stress on the strength of the rock mass. In the cases that effects of the intermediate principle stress are ignored, the value of b is equal to zero (USC coincides with Hoek-Brown failure criterion), while larger values reflect the effects of different extents of intermediate principle stress. Five common b values, 0, 0.25, 0.5, 0.75 and 1, are used to investigate the role of intermediate principle stress on the ground reaction curve. In this regard, re-modeling the case of Zareifard and Fahimifar (2016) (Section 6.1.3), as shown in Fig. 13, it is declared that considering the b parameter will affect the ground reaction curve. It should be taken into the consideration that other incorporating parameters are constant and equal to the original case of Zareifard and Fahimifar (2016). As shown, ignoring the intermediate principle stress parameter leads to overestimating displacements and hence the support system. Also, with increasing the values of b, tunnel's convergence, radial displacement, decreases. It is due to the fact that strength of the surrounding rock mass increases, as other missing rock mass' strength index is incorporated into the model.

5.4.2. Effect of weight of the damaged rock mass in EDZ

Similar to the previous section, the case of Zareifard and Fahimifar (2016) is re-modeled using the new proposed solution and considering the effect of the weight of the damaged zone. Assuming $\gamma^{'} = 30(kN/m^3)$, two different radiuses, 7 (m) (similar to the original case of Zareifard and Fahimifar (2016)) and 8 (m), for the damaged zone are assumed. Also, effect of both of constant and variable Young's modulus on the ground reaction curve is investigated. Indeed, in the case of variable Young's modulus, it is subjected to a linear decrease from the available value for the elastic mass, 5500 MPa, to the proposed value of Hoek and Diederichs (2006) for the damaged mass at the tunnel boundary, 2567 MPa and the obtained results are compared to the case of a constant Young's modulus, 3800 MPa, for the whole damaged zone. As shown in Fig. 14, considering a variable Young's modulus results in

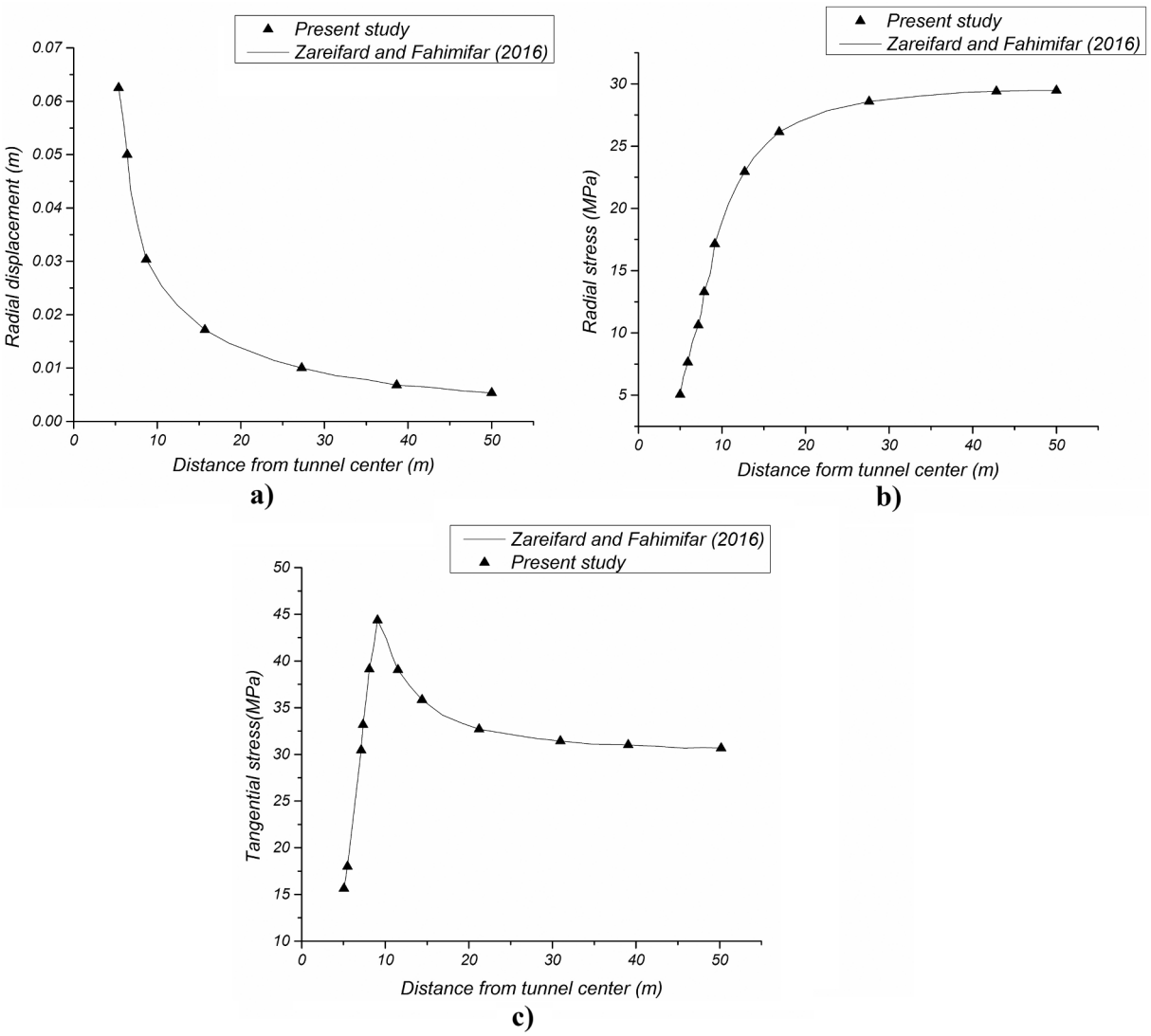

Fig. 12. Comparison with (a) radial displacements; (b) radial stresses and (c) tangential stresses of Zareifard and Fahimifar (2016); soft rock mass case; $R_{EDZ} = 7m$.

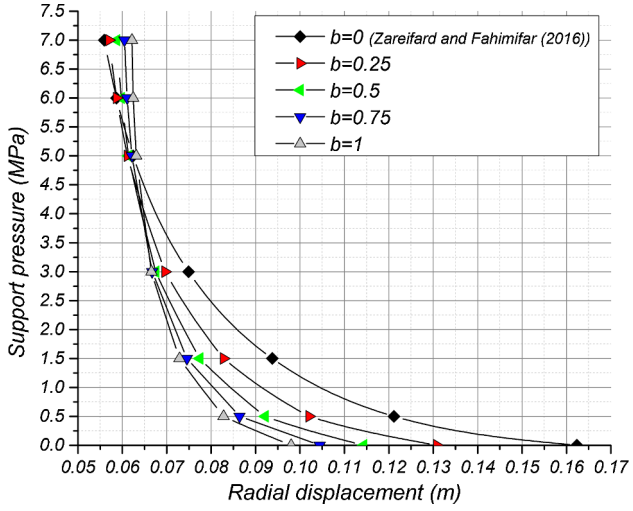

Fig. 13. Effect of intermediate principle stress on the ground reaction curve.

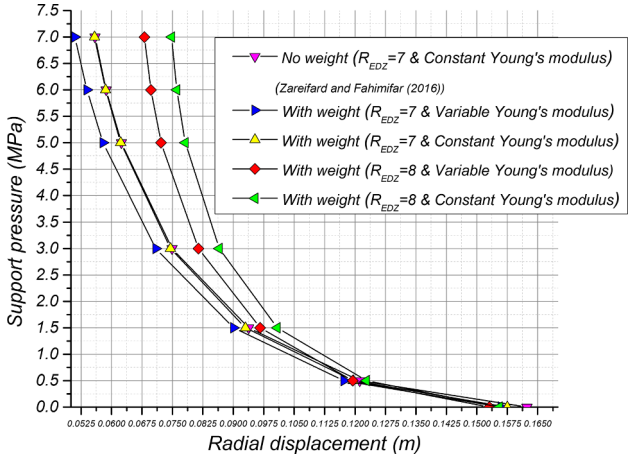

Fig. 14. Effect of weight of damaged zone on the radial stresses around the tunnel in the crown direction.

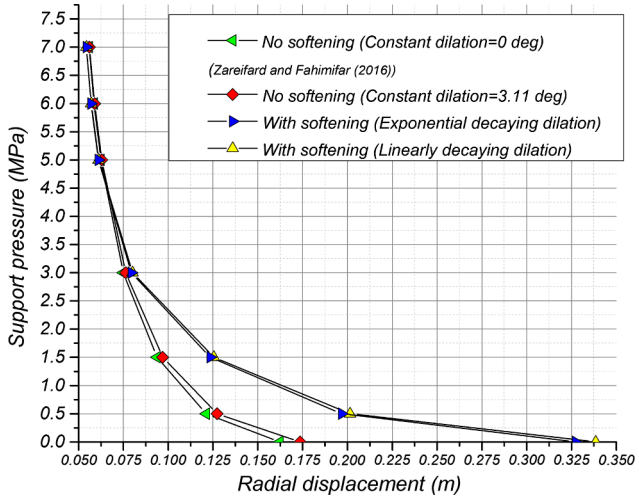

Fig. 15. Effect of dilation parameter on the ground reaction curve.

lower displacements for a defined support pressure. Also, for low support pressures, consideration of the weight of the damaged zone and increasing its radius results in almost the same displacements. On the other hand, for higher support pressures, larger radial displacements are occurred when higher weights of the damaged zone are introduced to the problem.

5.4.3. Effect of exponential decaying dilation and critical softening parameter

As described in Section 6.1.3, the studied material is a medium rock mass and hence, an elastic-plastic behavior, which considers the material's softening better presents the material's accurate behavior. Hereupon, in this section, effects of deterioration of material's strength parameters (material softening) is evaluated. Also, in the case of Zareifard and Fahimifar (2016), a constant dilation parameter is used to characterize stress-strain relationships around the tunnel. However, (Alejano and Alonso, 2005) recommended the application of an exponential decaying dilation parameter in the development of post-peak behavior of rock masses in the plastic region. Regarding the proposed methodology and the developed algorithm, Fig. 15 applies the original data presented in Zareifard and Fahimifar (2016) and compares different dilation behaviors. In this regard, similar to the original solution, the first model assumes a constant dilation parameter (no material softening is allowed and two different values for Ψ_p are investigated; 0° (similar to the original case of Zareifard and Fahimifar (2016)) and 3.11°), while similar to Lee and Pietruszczak (2008), the second solution considers a linear decrease in the dilation angle (it considers a linear decrease in the dilation angle (regarding Eqs. (17) and (18)) and updates the dilation parameter regarding Eq. (8) for Ψ_i values instead of Ψ_p). The third model (considering that all other concerning parameters are kept constant) incrementally updates (with an exponential decaying trend with respect to the softening parameter) values of k_i based on the initial k_p available on the softening-residual boundary (based on $\Psi_p = 3.11^{\circ}$). Fig. 15 shows how the tunnel behavior is influenced by different dilation behaviors. It should be noted that values of Ψ_p (used in the second and third models) and Ψ_r (used in the second model) are, respectively, 3.11° and 2.44°. Their values are calculated using Eqs. (9) and (10) (in Eqs. (9) and (10), residual parameters are used to obtain the residual dilation angle). In addition, strength parameters of the rock mass in the residual region are computed using Eq. (21) and the proposed relationships for the calculation of Hoek-Brown strength parameters ($m_r = 0.805$, $s_r = 0.00039$ and $a_r = a^{'} = 0.523$). Other affecting parameters are kept constant.

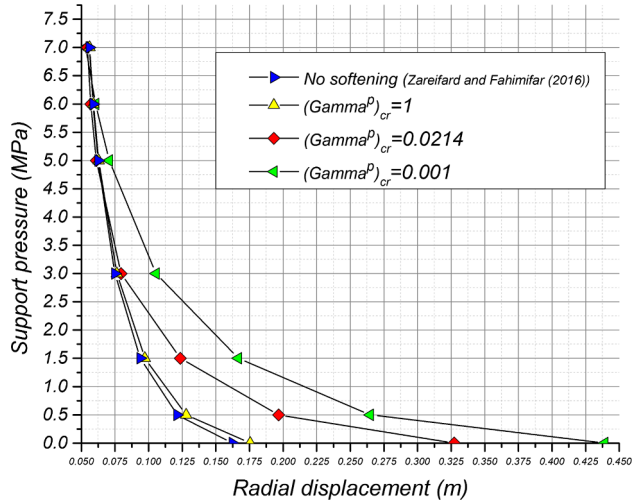

Fig. 16. Effect of critical softening parameter on the ground reaction curve.

As depicted in Fig. 15, in the cases that materials' softening behavior is not allowed, tunnel's convergence is underestimated. Increasing the occurred displacements in the softening models is a consequence of deterioration of material's peak strength parameters to the residual ones. Also, radial displacement of tunnel's crown increases as the constant dilation angle increases. In addition, comparing to the exponential decaying dilation model, the second softening model, linearly decaying dilation model, slightly overestimates displacements.

Moreover, to investigate the role of existing a softening zone on the ground reaction curve, three different critical softening parameters (0.001, 0.0214 and 1) are considered (for the exponential decaying dilation model) and the materials' strength parameters are subjected to a deterioration for softening parameters greater than these values and results are compared to the original case of Zareifard and Fahimifar (2016) (Fig. 16). It should be noted that the value of $\gamma^{p*} = 0.0214$ corresponds to the case of application of Eq. (18) to the original problem of Zareifard and Fahimifar (2016).

As Fig. 16 declares, tunnels surrounded by rock masses with higher critical softening parameters experience lower radial displacements. It can be due to increasing the rock masses' ductility and decreasing its brittleness as a consequence of increasing the critical softening parameter. Indeed, in such materials, the deterioration of material's strength parameters is later initiated (with respect to the softening parameter development).

6. Conclusion

A new method to solve stress-strain around circular tunnels surrounded by elastic-plastic-EDZ rock mass under far field hydrostatic stress is presented. Effect of intermediate principle stresses are also taken into account through the parameter b available in the Unified Strength Criterion (USC). The developed solution algorithm uses advantages of both well-derived solution schemes (variable dilation parameter of Alejano and Alonso (2005) and Alejano et al. (2009, 2010), as well as the iterative finite difference solution proposed by Lee and Pietruszczak (2008)). In this regard, the general solution scheme proposed by Lee and Pietruszczak (2008) is extended to account for the formation of excavation damaged zone around the tunnels. First, using the Runge-Kutta-Fehlberg numerical solution of the governing equilibrium equation, radial stress in the plastic-EDZ boundary is calculated and the solution steps are performed for the plastic region, considering the pre-defined value of critical support pressure (calculated using Newton-Raphson method) and a monotonic decrease of radial stress from P_{iC} to the value of radial stress in the plastic-EDZ boundary, σ_r^{P-E}. In the proposed algorithm, material softening (through defining softening parameter and softening-residual boundary) and exponentially decaying dilation parameter are both allowed in the plastic zone. Also,

dilation parameter can be assessed using both Mohr-coulomb and Hoek-Brown similar types of plastic potential functions. The obtained results for strains and stresses in the last iteration of the solution in the plastic region is used as an initial condition for the excavation damaged zone, and the solution is then followed by the monotonical decrease of radial stress form σ_r^{P-E} to internal support pressure, . While solving for stress-strain states in the damaged zone (separately for tunnel's crown and sidewalls' directions), variation of Young's modulus in EDZ proposed by Saiang (2008a), deterioration of material's strength parameters, and the weight of the damaged material are considered, and the normalized radius in this zone is calculated in a way so as to yield the governing equilibrium equation. Also, tangential plastic strain increments are calculated using the finite difference approximation of the compatibility equation in EDZ based on the newly developed normalized radius. It is used in conjunction with dilation parameter to achieve radial plastic strain increments based on the non-associative flow rule. Following the described algorithm, the pressures required to restrict the tunnel's displacements to arbitrary u_i, ground reaction curve, are obtained. To approve the validity of the proposed approach, results of the field measurements of Hanlingjie tunnel in China is used. Comparing the obtained results to the field measurements in the tunnel's crown, its accuracy is proven. In addition, the comprehensiveness of the proposed solution is examined through three simplified cases. In these examples, the problem is simplified to the cases that have closed-form or numerical solutions available in the literature. It is shown that the results of the simplified solution comply well with the ground reaction curve, stresses and strains of the available solutions. It should be noted that modeling all the concerning parameters will possibly result in considerable differences in the developed GRCs. To show the described discrepancy, the case of Zareifard and Fahimifar (2016) is selected for further investigations. Applying new features of the proposed algorithm to the original model of Zareifard and Fahimifar (2016), effects of new different introduced parameters on the ground reaction curve is evaluated. It is shown that intermediate principle stress, exponential decaying dilation, critical softening parameter and the weight of the damaged zone considerably affect the GRC of the tunnel in an elastic-plastic-EDZ rock mass and ignoring these parameters will result in significant discrepancies in the ground reaction curves.

The proposed method can be efficiently used to comprehensively model the ground reaction curve of circular tunnels in the medium quality rock masses. In addition, parametric studies to account for uncertainties in the damaged zone will be carried out considerably more efficiently using the new method as compared to available commercial FEM, FDM, and BEM numerical packages (from both time-saving and cost-effectiveness points of view).

Appendix A. Supplementary material

Supplementary data to this article can be found online at https://doi.org/10.1016/j.tust.2018.11.045.

References

Abbasi, B., Pierce, M., Dzik, E., Chugh, Y., 2014. Barton approach for predicting Hoek-Brown residual parameters. s.l., s.n., pp. ARMA-2014-7634.

Alejano, L., Alonso, E., 2005. Considerations of the dilatancy angle in rocks and rock masses. Int. J. Rock Mech. Min. Sci. 42, 481–507.

Alejano, L., Alonso, E., Rodriguez-Dono, A., Fdez-Manin, 2010. Application of the convergence-confinement method to tunnels in rock masses exhibiting Hoek-Brown strain-softening behavior. Int. J. Rock Mech. Min. Sci. 47, 150–160.

Alejano, L., Rodriguez-Dono, A., Alonso, E., Fdez-Manin, G., 2009. Ground reaction curves for tunnels excavated in different quality rock masses showing several types of post-failure behavior. Tunn. Undergr. Space Technol. 24, 689–705.

Alejano, L., Rodriguez-Dono, A., Veiga, M., 2012. Plastic Radii and longitudinal deformation profiles of tunnels excavated in strain-softening rock masses. Tunn. Undergr. Space Technol. 30, 169–182.

Alonso, E., et al., 2003. Ground response curves for rock masses exhibiting strain-softening behavior. Int. J. Numer. Anal. Meth. Geomech. 27, 1153–1185.

Andersson, P., 1992. Excavation Disturbed Zone in Tunneling. Swedish Rock Engineering Research, Stockholm.

Anläggnings AMA 98, 1999. General materials and works description for construction work section CBC: Bergschakt, Stokholm: Svensk Byggtjänst.

Azadi, M., Hosseini, S., 2010. Analyses of the effect of seismic behavior of shallow tunnels in liquefiable grounds. Tunn. Undergr. Space Technol. 25 (5), 543–552.

Brown, E., Bray, J., Ladanyi, B., Hoek, E., 1983. Ground response curves for rock tunnels. J. Geotech. Eng. 109 (1), 15–39.

Carranza-Torres, C., Fairhurst, C., 1999. The elasto-plastic response of underground excavations in rock masses that satisfy the Hoek-Brown failure criterion. Int. J. Rock Mech. Min. Sci. 36, 777–809.

Carranza-Torres, C., Fairhurst, C., 2000. Application of the convergence-confinement method of tunnel design to rock masses that satisfy the Hoek-Brown failure criterion. Tunn. Undergr. Space Technol. 15 (2), 187–213.

Chapra, S., Canale, R., 2002. Numerical Methods for Engineers, fourth ed. McGraw-Hill, New York.

Clausen, J., 2007. Efficient non-linear finite element implementation of elasto-plasticity for geotechnical problems. Ph.D. Thesis ed. 8, 6700 Esbjerg, Denmark: Faculty of Engineering, Science and Medicine, Aalborg University, Esbjerg Institute of Technology.

Fahimifar, A., Ghadami, H., Ahmadvand, M., 2014. The influence of seepage and gravitational loads on elastoplastic solution of circular tunnels. Scientia Iranica A 21 (6), 1821–1832.

Florence, A., Schwer, L., 1978. Axisymmetric compression of a Mohr-Coulomb medium around a circular hole. Int. J. Numer. Anal. Meth. Geomech. 2, 367–379.

García-Bastante, F., Alejano, L., González-Cao, J., 2012. Predicting the extent of blast induced damage in rock masses. Int. J. Rock Mech. Min. Sci. 56, 44–53.

Ghorbani, A., Hasanzadehshooiili, H., 2017. A novel solution for ground reaction curve of tunnels in elastoplastic strain softening rock masses. J. Civil Eng. Manage. 23 (6), 773–786.

Ghorbani, A., Hasanzadehshooiili, H., Sadowski, L., 2018. Neural prediction of tunnels' support pressure in elasto-plastic, strain-softening rock mass. Appl. Sci. 8 (5), 841.

Ghorbani, A., Hasanzadehshooiili, H., Šapalas, A., Lakirouhani, A., 2013. Buckling of the steel liners of underground road structures: the sensitivity analysis of geometrical parameters. Baltic J. Road Bridge Eng. 8 (4), 250–254.

González-Cao, J., Varas, F., Bastante, F., Alejano, L., 2013. Ground reaction curves for circular excavations in non-homogeneous, axisymmetric strain-softening rock masses. J. Rock Mech. Geotech. Eng. 5, 431–442.

Guan, Z., Jiang, Y., Tanabasi, Y., 2007. Ground reaction analyses in conventional tunnelling excavations. Tunn. Undergr. Space Technol. 22, 230–237.

Hamdi, P., Stead, D., Elmo, D., 2014. Damage characterization during laboratory strength testing: A 3D-finite-discrete element approach. Comput. Geotech. 60, 33–46.

Hasanzadehshooiili, H., Lakirouhani, A., Medzvieckas, J., 2012. Evaluating elastic-plastic behaviour of rock materials using Hoek-Brown failure criterion. J. Civil Eng. Manage. 18 (3), 402–407.

Hoek, E., 2012. Blast damage factor D, s.l.: Technical note for Rocscience.

Hoek, E., Brown, E., 1997. Practical estimates of rock mass strength. Int. J. Rock Mech. Min. Sci. 34, 1165–1181.

Hoek, E., Carranza-Torres, C., Corkum, B., 2002. Hoek-Brown failure criterion-2002 edition. Toronto, Ontario, Canada, s.n., pp. 267–273.

Hoek, E., Diederichs, M., 2006. Empirical estimation of rock mass modulus. Int. J. Rock Mech. Min. Sci. 43 (2), 203–215.

Holmberg, R., Persson, P.-A., 1980. Design of tunnel perimeter blasthole patterns to prevent rock damage. Transc. Inst. Min. Metall. A37–A40.

Huang, F., Zhu, H., Jiang, S., Liang, B., 2016. Excavation-damaged zone around tunnel surface under different release ratios of displacement. Int. J. Geomech.

Hustrulid, W., Bennet, R., Ashland, F., Lenjani, M., 1992. A new method for predicting the extent of the blast damage zone. s.l., Nitro Nobel Gyttorp, p. Paper No. 3.

Katzenbach, R., et al., 2013. Soil-structure-interaction of tunnels and superstructures during construction and service time. Procedia Eng. 57, 35–44.

Ketabian, E., Molladavoodi, H., 2015. Practical ground response curve considering post-peak rock mass behavior. Eur. J. Environ. Civil Eng.

Kolymbas, D., 2005. Tunnelling and Tunnel Mechanics. Springer-Verlag, Berlin Heidelberg.

Lee, Y., Pietruszczak, S., 2008. A new numerical procedure for elasto-plastic analysis of a circular opening excavated in a strain-softening rock mass. Tunn. Undergr. Space Technol. 23, 588–599.

Mathews, J., Fink, K., 2004. Numerical Methods using Matlab, fourth ed. Prentice-Hall Inc., USA.

Mitaim, S., Detournay, E., 2005. Determination of ground reaction curve for hyperbolic soil model using the hodograph method. Can. Geotech. J. 42, 964–968.

Mohammadi, E., Fahimifar, A., 2015. Elastoplastic analysis of the tunnel considering the nonlinear relations of the strength parameters from peak to residual in the strain softening stage. Modares Civil Eng. J. 14 (4), 171–178.

Mohammadi, H., Farsangi, M., Jalalifar, H., Ahmadi, A., 2013. Influence of gravity loading on the grond reaction curve at tunnel crown based on the nonlinear Unified strength criterion. Int. Res. J. Appl. Basic Sci. 6 (5), 563–571.

Nyberg, U., Fjellborg, S., Olsson, M., Ouchterlony, F., 2000a. Judging blast damage in drfit perimeters, Sweden: s.n.

Nyberg, U., Fjellborg, S., Olsson, M., Ouchterlony, F., 2000b. Vibration Measurements, Damage Prediction and Crack Mapping in Magnetite Ore and Waste Rock. sh Rock Engineering Research, Stockholm.

Olsson, M., et al., 2004. Äspö HRL: Experiences of Blasting of the TASQ Tunnel. SKB, Stockholm.

Olsson, M., Bergqvist, I., 1993. Crack Lengths from Explosives in Small Diameter Holes. Swedish Rock Engineering Research, Stockholm.

Olsson, M., Bergqvist, I., 1995. Crack Propagation in Rock from Multiple Hole Blasting - Part 1. Swedish Rock Engineering Research, Stockholm.

Olsson, M., Bergqvist, I., 1997. Crack Propagation in Rock from Multiple Hole Blasting - Summary of Work During the Period 1993–96. Swedish Rock Engineering Research, Stockholm.

Olsson, M., Bergqvist, I., Ouchterlony, F., 2002. The Influence of Shock Wave and Gas

Pressure on Blast Induced Cracks. Swedish Rock Engineering Research, Stockholm.
Olsson, M., Ouchterlony, F., 2003. New Formula for Blast Induced Damage in the Remaning Rock. Swedish Rock Engineering Research, Stockholm.
Park, K., 2014. Similarity solution for a spherical or circular opening in elastic-strain softening rock mass. Int. J. Rock Mech. Min. Sci. 71, 151–159.
Park, K., 2015. Large strain similarity solution for a spherical or circular opening excavated in elastic-perfectly plastic media. Int. J. Numer. Anal. Meth. Geomech. 39 (7), 724–737.
Park, K., Tontavanich, B., Lee, J., 2008. A simple procedure for ground response of circular tunnel in elastic-strain softening rock masses. Tunn. Undergr. Space Technol. 23, 151–159.
Saiang, D., 2008a. Behaviour of blast-induced damaged zone around underground excavations in hard rock mass. Ph.D. Dissertation ed. Sweden: Division of Rock Mechanics, Department of Civil, Mining and Environmental Engineering, Lulea University of Technology.
Saiang, D., 2008b. Blast-induced damage: summary of SVEBEFO investigations, s.l.: s.n.
Serrano, A., Olalla, C., Reig, I., 2011. Convergence of circular tunnels in elastoplastic rock masses with non-linear failure criteria and non-associated flow laws. Int. J. Rock Mech. Min. Sci. 48, 878–887.
Sharan, S., 2008. Analytical solutions for stress & displacements around a circular opening in a generalized Hoek-Brown rock. Int. J. Rock Mech. Min. Sci. 45, 78–85.
Veiskarami, M., Ghorbani, A., Alavipour, M., 2012. Development of a constitutive model for rockfills and similar granular materials based on the distributed state concept. Frontiers Struct. Civil Eng. 6, 365–378.
Vrakas, A., Anagnostou, G., 2014. A finite strain closed-form solution for the elastoplastic ground response curve in tunneling. Int. J. Numer. Anal. Meth. Geomech. 38 (11), 1131–1148.
Wang, S., Yin, S., 2011. A closed-form solution for a spherical cavity in the elastic-brittle-plastic medium. Tunn. Undergr. Space Technol. 26, 236–241.
Wang, S., Yin, X., Tang, H., Ge, X., 2010. A new approach for analyzing circular tunnel in strain-softening rock masses. Int. J. Rock Mech. Min. Sci. 47 (1), 170–178.
Xu, S., Yu, M., 2006. The effect of the intermediate principal stress on the ground response of circular openings in rock mass. Rock Mech. Rock Eng. 39 (2), 169–181.
Yu, M., Zan, Y., Zhao, J., Yoshimine, M., 2002. A unified strength criterion for rock materials. Int. J. Rock Mech. Min. Sci. 39 (8), 975–989.
Zareifard, M., Fahimifar, A., 2012. A new solution for shallow and deep tunnels by considering the gravitional loads. Acta Geotech. Slovenica 2, 37–49.
Zareifard, M., Fahimifar, A., 2014. Elastic-brittle-plastic analysis of circular deep underwater cavities in a Mohr-Coulomb rock mass considering seepage forces. Int. J. Geomech.
Zareifard, M., Fahimifar, A., 2016. Analytical solutions for the stresses and deformations of deep tunnels in an elastic-brittle-plastic rock mass considering the damaged zone. Tunn. Undergr. Space Technol. 58, 186–196.
Zhang, C., et al., 2010. Unified analytical solutions for a circular opening based on nonlinear unified failure criterion. J. Zhejiang Univ.-Sci. A (Appl. Phys. Eng.) 11 (2), 71–79.
Zhang, C., Zhao, J., Zhang, Q., Hu, X., 2012. A new closed-form solution for circular openings modeled by the Unified strength theory and radius-dependent Young's modulus. Comput. Geotech. 42, 118–128.
Zhang, Z., et al., 2017. Analytical prediction for ground movements and liner internal dorces induced by shallow tunnels considering non-uniform convergence pattern and ground-liner interaction mechanism. Soils Found 57 (2), 211–226.
Zou, J.-F., Li, C., Wang, F., 2017. A new procedure for ground response curve (GRC) in strain-softening surronding rock. Comput. Geotech. 89, 81–91.